Journal of Sound and Vibration 399 (2017) 285–307

Contents lists available at ScienceDirect

Journal of Sound and Vibration

journal homepage: www.elsevier.com/locate/jsvi

Structural damage detection by a new iterative regularization method and an improved sensitivity function

Alireza Entezami, Hashem Shariatmadar*, Hassan Sarmadi

Department of Civil Engineering, Faculty of Engineering, Ferdowsi University of Mashhad, Mashhad, Iran

ARTICLE INFO

Article history:
Received 2 February 2016
Received in revised form
23 January 2017
Accepted 14 February 2017
Handling Editor: I. Trendafilova
Available online 14 April 2017

Keywords:
Structural damage detection
Model updating
Sensitivity analysis
Modal strain energy
Iterative regularization method
Incomplete noisy modal data

ABSTRACT

A new sensitivity-based damage detection method is proposed to identify and estimate the location and severity of structural damage using incomplete noisy modal data. For these purposes, an improved sensitivity function of modal strain energy (MSE) based on Lagrange optimization problem is derived to adapt the initial sensitivity formulation of MSE to damage detection problem with the aid of new mathematical approaches. In the presence of incomplete noisy modal data, the sensitivity matrix is sparse, rectangular, and ill-conditioned, which leads to an ill-posed damage equation. To overcome this issue, a new regularization method named as Regularized Least Squares Minimal Residual (RLSMR) is proposed to solve the ill-posed damage equation. This method relies on Krylov subspace and exploits bidiagonalization and iterative algorithms to solve linear mathematical systems. For the majority of Krylov subspace methods, conventional direct methods for the determination of an optimal regularization parameter may not be proper. To cope with this limitation, a hybrid technique is introduced that depends on the residual of RLSMR method, the number of iterations, and the bidiagonalization algorithm. The accuracy and performance of the improved and proposed methods are numerically examined by a planner truss by incorporating incomplete noisy modal parameters and finite element modeling errors. A comparative study on the initial and improved sensitivity functions is conduced to investigate damage detectability of these sensitivity formulations. Furthermore, the accuracy and robustness of RLSMR method in detecting damage are compared with the well-known Tikhonov regularization method. Results show that the improved sensitivity of MSE is an efficient tool for using in the damage detection problem due to a high sensitivity to damage and reliable damage detectability in comparison with the initial sensitivity function. Additionally, it is observed that the RLSMR method with the aid of the hybrid technique successfully solves the ill-posed damage equation and provides better damage detection results compared with the Tikhonov regularization technique.

1. Introduction

Many existing civil engineering infrastructures were constructed several decades ago, which are still in service despite of their age and structural weakness. Deterioration and damage of these structures may cause irrecoverable economic losses,

* Corresponding author.
E-mail addresses: entezami@mail.um.ac.ir (A. Entezami), shariatmadar@um.ac.ir (H. Shariatmadar), hassan.sarmadi@alumni.um.ac.ir (H. Sarmadi).

http://dx.doi.org/10.1016/j.jsv.2017.02.038
0022-460X/

human injuries, and death. In order to prevent such undesirable issues, many attempts have been performed by researchers and engineers in the context of structural health monitoring (SHM) to assess the integrity of structures and detect any probable structural damage. Damage in a structure can occur with deviations in geometry configurations, boundary conditions, and deterioration of materials leading to cracks in concrete, loose bolts and broken welds in steel connections, corrosions, and fatigue. These adverse changes may cause undesirable stresses and displacements, unfavorable vibrations, failure and even collapse. The process of damage identification by vibration data is usually known as vibration-based damage detection, which is categorized into four levels including damage existence (level 1), damage localization (level 2), damage quantification (level 3), and damage prognosis (level 4) [1]. The primary idea behind vibration-based damage detection methods is that structural damage leads to inappropriate changes in the inherent physical properties of a structure such as mass, stiffness, and damping. Any deviation in these properties, therefore, changes dynamic characteristics or vibration responses of the structure.

Even though many innovative vibration-based methods have been proposed more recently, modal-based approaches are still widely used in the problem of damage detection. The underlying reason is that the modal parameters such as natural frequencies and mode shapes depend directly on the inherent physical properties regardless of the excitation sources. Some of these methods use direct changes in the natural frequencies [2,3] and mode shapes [4–6] for structural damage detection. However, the modal frequencies provide only global information about the condition of structure and typically fail to locate damage [7]. The modal displacements or mode shapes, on the other hand, are usually more difficult to measure accurately and are not extremely sensitive to moderate changes in structural stiffness [8].

Sensitivity-based damage detection methods using the modal parameters are other kinds of approaches relying on the sensitivity analysis of measurable dynamic outputs of the structure. The sensitivity analysis represents how dynamic characteristics vary based on changes in the physical properties of the structure [9]. A variety of methods have been developed to derive the sensitivity of modal parameters that can be found some of them in [10–13]. Additionally, the sensitivity of modal strain energy (MSE) is another efficient and useful sensitivity function that can be much more sensitive to damage. Various methods have been presented to establish different sensitivity formulations of MSE based on the direct difference and algebraic methods, the indirect methods, and the variation principle. Yan and Ren [14] proposed a direct algebraic method to determine the sensitivity of MSE for a real symmetric undamped system. Yan et al. [15] presented a statistic structural damage detection algorithm using the sensitivity of MSE for the process of damage detection based on ambient vibration measurements, where operational mode shapes is the only available data. Li et al. [16] proposed a sensitivity function of MSE using the variation principle in order to design structural parameters by Lagrange function.

An important issue regarding the sensitivity-based methods is to derive a well-established sensitivity function. For the damage detection problem, in general, the sensitivity formulation should be sensitive to damage. A salient characteristic of a well-established sensitivity function is damage detectability without applying any complicated mathematical techniques to solve damage equations. Furthermore, the incompleteness conditions of modal parameters provide limitations of using the sensitivity-based methods in detecting damage. In practice, there is no necessity to measure all modal frequencies from dynamic tests, because in the large-scale structures only low-order natural frequencies are measureable. As another limitation, the number of measured modes is normally less than the number of degrees of freedom (DOFs) resulting from practical and economic limitations of installing sensors at all DOFs. Under such circumstances, the sensitivity matrix gained by incomplete modal parameters may be sparse, rectangular, and ill-conditioned. Measurement errors in vibration response data are other obstacle to achieve successful damage detection results, because both measurement errors and ill-conditioned sensitivity matrix lead to an ill-posed damage equation [17]. This means that conventional mathematical methods based on inverse problems are not robustly able to solve an ill-posed problem.

To cope with this shortcoming, regularization methods are in general applied to guarantee the existence, uniqueness, and stability of the solution of ill-posed damage equation. The regularized solution of damage identification problem can be found in the article of Chen [18], who utilized a regularization method, truncated singular value decomposition (TSVD), for detecting damage in a 16-story braced frame building model. Weber et al. [19] applied Tikhonov regularization and TSVD methods to detect structural damage in a full-scale laboratory concrete frame. Li and Law [20] proposed an adaptive Tikhonov regularization approach for damage detection based on solving a nonlinear model updating inverse problem. In another research, Chen and Maung [21] presented a direct model updating method using dynamic perturbation theory of structural parameters and incomplete noisy modal data. For a regularized solution, they utilized Tikhonov regularization method along with the L-curve method for the determination of regularization parameter. Another application of regularized solution to vibration-based problems can be found in Aucejo [22], who introduced Generalized Iteratively Reweighted Least-Squares (GIRLS) algorithm to solve a generalized Tikhonov regularization problem for the identification of force sources using vibration measurements. Grip et al. [23] investigated a new regularization method based on the minimization of total variation for the damage detection problem based on the sensitivity-based model updating strategy. In their article, they compared the new regularization method with a well-established interpolation-based regularization approach.

Despite many research efforts in vibration-based methods using sensitivity functions and regularization techniques, one of the critical and challenging issues is how to robustly deal with the ill-posed problem with the sparse and ill-conditioned sensitivity matrix. Another prominent issue is to use a well-established sensitivity function regarding the damage detection problem. As a result, the main objective of this article is to propose a new sensitivity-based damage detection method using incomplete noisy modal data for locating damage and quantifying damage severity. To achieve these aims, the initial sensitivity function of MSE proposed by Li et al. [16] is enhanced to establish a new sensitivity formulation pertinent to damage. The improved formulation is based on Lagrange optimization problem by developing constraints and applying new mathematical approaches for the calculation of Lagrange multipliers. A well-known mode expansion technique is used to overcome the use of incomplete measured mode shapes in the formulations regarding the damage detection problem. A new iterative regularization method namely Regularized Least Squares Minimal Residual (RLSMR) is presented to solve an ill-posed damage identification equation in the presence of incomplete noisy modal parameters. This method is one of the Krylov subspace techniques, which exploits bidiagonalization and iterative algorithms to solve linear mathematical systems with a sparse and ill-conditioned sensitivity (coefficient) matrix. Due to the dependence of each regularization method on the regularization parameter, a hybrid method as a combination of a projection technique with a direct regularization method is introduced to determinate an optimal regularization value. This technique depends on the residual of RLSMR method, the number of iterations, and the bidiagonalization algorithm. Eventually, the effectiveness and reliability of the improved and proposed methods are numerically verified by a planner truss. A comparative study on the initial and improved sensitivity functions is conduced to assess the damage detectability of these functions. As another comparative study, the robustness and accuracy of RLSMR method in detecting structural damage are compared with the well-known Tikhonov regularization method. Results demonstrate that the improved sensitivity of MSE is sensitive to damage in comparison with the initial sensitivity function. In addition, the RLSMR method along with the hybrid technique is successful in damage localization and quantification. Additionally, this method provides better results compared to the Tikhonov regularization method, when the sparse and ill-conditioned sensitivity matrix as well as the incomplete noisy modal parameters are available.

2. Theoretical background

2.1. Basic dynamic equations

For an n DOFs structural system, the equation of motion for free vibration leads to the following eigenvalue problem:

$$\left(\mathbf{K} - \lambda_i \mathbf{M}\right)\boldsymbol{\varphi}_i = 0 \tag{1}$$

where $\mathbf{K}\in\Re^{n\times n}$ and $\mathbf{M}\in\Re^{n\times n}$ are the stiffness and mass matrices of the structural system; λ_i and $\boldsymbol{\varphi}_i$ represent the ith eigenvalue (the square of natural frequency) and eigenvector (mode shape), respectively. Assume that the eigenvectors are mass-normalized; hence, the mass and stiffness orthogonality conditions are expressed as:

$$\boldsymbol{\varphi}_i^T \mathbf{M}\boldsymbol{\varphi}_i = 1 \tag{2}$$

$$\boldsymbol{\varphi}_i^T \mathbf{K}\boldsymbol{\varphi}_i = \lambda_i \tag{3}$$

When the vectors of mode shape are equivalent to the nodal displacements in a structure, strain energy is stored in each structural element. The strain energy in a structure is known as modal strain energy, which can be used as a valuable dynamic characteristic in vibration-based applications. The sensitivity of MSE can be applied to system identification, sensitivity design analysis, finite element model updating, structural design optimization, and damage detection. For the i^{th} mass-normalized mode shape, the global MSE is formulated as a combination of global stiffness matrix and mode shape in the following form:

$$\mathbf{MSE}_i = \frac{1}{2}\boldsymbol{\varphi}_i^T \mathbf{K}\boldsymbol{\varphi}_i \tag{4}$$

Assume that the global stiffness matrix is composed of ne local stiffness matrices of individual elements. On this basis, the j^{th} element of MSE is given by:

$$\mathbf{MSE}_{ji} = \frac{1}{2}\sum_{j=1}^{\boldsymbol{ne}} \boldsymbol{\varphi}_i^T \mathbf{k}_j \boldsymbol{\varphi}_i \tag{5}$$

where $\mathbf{k}_j$ represents the local stiffness matrix at the j^{th} element $\left(\mathbf{K} = \sum_{j=1}^{ne}\mathbf{k}_j\right)$.

2.2. Mass-normalization of measured mode shapes

In order to use both analytical and experimental mode shapes in vibration-based applications, the mode shapes of FE and real structures should be the same physical condition [9]. Therefore, it is indispensable to scale the measured modal displacements with the mass-normalized analytical mode shapes. Assume that $\hat{\boldsymbol{\psi}}_i$ represents the i^{th} unscaled mode shape measured at a few DOFs. The mass-normalized incomplete measured mode shape $\hat{\boldsymbol{\varphi}}_i^m$ is obtained by:

$$\hat{\boldsymbol{\varphi}}_i^m = \nu_i \hat{\boldsymbol{\psi}}_i \tag{6}$$

in which the mode scale factor ν_i is defined as:

$$\nu_i = \frac{\boldsymbol{\varphi}_i^{m^T}\hat{\boldsymbol{\psi}}_i}{\hat{\boldsymbol{\psi}}_i^T\hat{\boldsymbol{\psi}}_i} \tag{7}$$

where $\boldsymbol{\varphi}_i^m$ denotes the i[th] analytical mode shape restricted to the same dimensions as $\hat{\boldsymbol{\psi}}$. It is important to mention that the full set of analytical mode shape is generally divided into two complementary sets, including the measured (master) mode shape ($\boldsymbol{\varphi}^m$) and the remaining unmeasured (slave) mode shape ($\boldsymbol{\varphi}^u$) [24,25].

2.3. Mode expansion strategy

In reality, it is not possible to measure all modal displacements at all DOFs resulting from some practical and economic limitations. Therefore, the measured mode shapes from a dynamic test are normally incomplete and only exist at a few DOFs. In this case, a crucial issue arises how to use the measured incomplete mode shapes in the majority of formulations. Model reduction or mode expansion techniques are normally applied to address this problem [26]. For damage detection problems, it is necessary to use a complete structure model with detailed damage characterization in order to correctly detect structural damage at detailed level [18]. On this basis, it would be preferable to applying the mode expansion strategy instead of the model reduction approach [24,25]. General expansion techniques consist of the static expansion or Guyan method [27], the dynamic expansion method [28], and System Equivalent Reduction Expansion Process (SEREP) method [29]. In this article, the SEREP method is used to expand the measured mode shapes. The transformation matrix of this method is written as:

$$\mathbf{T}_{\mathbf{SEREP}} = \begin{bmatrix} \boldsymbol{\varphi}^m \\ \boldsymbol{\varphi}^u \end{bmatrix} \left(\boldsymbol{\varphi}^{m^T}\boldsymbol{\varphi}^m\right)^{-1}\boldsymbol{\varphi}^{m^T} \tag{8}$$

Consequently, the i[th] full measured mode shape of the tested structure $\hat{\boldsymbol{\varphi}}_i$, including the measured normalized part $\hat{\boldsymbol{\varphi}}_i^m$ and the unmeasured part $\hat{\boldsymbol{\varphi}}_i^u$, are obtained in the following form:

$$\hat{\boldsymbol{\varphi}}_i = \begin{bmatrix} \hat{\boldsymbol{\varphi}}_i^m \\ \hat{\boldsymbol{\varphi}}_i^u \end{bmatrix} = \mathbf{T}_{\mathbf{SEREP}}\hat{\boldsymbol{\varphi}}_i^m \tag{9}$$

3. An improved sensitivity function of modal strain energy

The sensitivity function of MSE refers to the calculation of the first-order derivative of MSE with respect to the structural parameter, p_j, which can be described as follows:

$$\frac{dMSE_{ji}}{dp_j} = \frac{1}{2}\left(\left(\frac{d\boldsymbol{\varphi}_i}{dp_j}\right)^T k_j\boldsymbol{\varphi}_i + \boldsymbol{\varphi}_i^T\mathbf{k}_j\frac{d\boldsymbol{\varphi}_i}{dp_j} + \boldsymbol{\varphi}_i^T\frac{d\mathbf{k}_j}{dp_j}\boldsymbol{\varphi}_i\right) \tag{10}$$

In general, Eq. (10) represents a direct sensitivity function of MSE, because it only needs the calculation of the first-order derivatives of mode shape and structural stiffness. The derivative of mode shape cannot be directly determined due to the fact that it requires to overcome the singular problem [16]. Another reason is that the first-order derivative of mode shape is intensively sensitive to small measurement errors available in the majority of vibration response data. Therefore, the direct or indirect applications of this derivative may not lead to a robust and compact sensitivity formulation of MSE. One novel way to establish an influential sensitivity function is to use the properties of Lagrange multipliers method based on the constrained optimization problem.

3.1. Lagrange multipliers method

The method of Lagrange multipliers is an equality-constrained optimization problem that attempts to maximize or minimize an objective function with some constraints [30,31]. A constrained optimization problem is a mathematical formulation according to the maximization or minimization of the objective function F subjected to the equality constraint G = 0 [32]. Both objective function and constraint consist of nv unknown variables, $x_1 \ldots x_{nv}$, which are usually described as design variables [31]. With these definitions, Lagrange function (L) is expressed as follows:

$$L\left(\boldsymbol{x}_1, \boldsymbol{x}_2, \ldots, \boldsymbol{x}_{\boldsymbol{nv}}, \theta_1, \theta_2, \ldots, \theta_{\boldsymbol{nm}}\right) = F(\boldsymbol{x}_1, \boldsymbol{x}_2, \ldots, \boldsymbol{x}_{\boldsymbol{nv}}) + \sum_{z=1}^{\boldsymbol{nm}} \theta_z G_z(\boldsymbol{x}_1, \boldsymbol{x}_2, \ldots, \boldsymbol{x}_{\boldsymbol{nv}}) \tag{11}$$

where $\theta_1 \ldots \theta_{nm}$ denote nm unknown Lagrange multipliers. By treating L as a function of $nv+nm$ unknowns, the necessary conditions for the solution of Lagrange function corresponding to the constrained optimization problem are given by:

$$\frac{\partial L}{\partial \boldsymbol{x}_v} = \frac{\partial F}{\partial \boldsymbol{x}_v} + \sum_{z=1}^{\boldsymbol{nm}} \theta_z \frac{\partial G_z}{\partial \boldsymbol{x}_v} = 0, \qquad v = 1, 2, \ldots, \boldsymbol{nv} \tag{12}$$

$$\frac{\partial L}{\partial \boldsymbol{\theta}_z} = G_z(\boldsymbol{x}_1, \boldsymbol{x}_2, \ldots, \boldsymbol{x}_{\boldsymbol{nv}}) = 0, \qquad z = 1, 2, \ldots, \boldsymbol{nm} \tag{13}$$

The solution of Eqs. (12) and (13) gives the unknown parameters of Lagrange function such as the variables $x_1, x_2, \ldots, x_{nv}$ and the Lagrange multipliers $\theta_1, \theta_2, \ldots, \theta_{nm}$. Definition of sufficient constraints for the Lagrange optimization problem is a crucial step, because if a critical constraint is not included in the formulation, the solution of optimization problem most likely to be unacceptable [32]. Moreover, the variables have to satisfy certain constraints to produce a reliable optimization solution implying the importance of choosing adequate constraints [31].

3.2. The initial sensitivity function

The initial sensitivity formulation of MSE based on the Lagrange multipliers method was proposed by Li et al. [16]. In their article, they dealt with the limitation of using the direct derivative of mode shape in the sensitivity function. The Lagrange function (L^*) in their work comprised an objection function (the element MSE), and two constraints including the eigenvalue problem and mass orthogonality condition. This function was defined as:

$$L^*(\boldsymbol{p}, \lambda_i, \boldsymbol{\varphi}_i) = MSE_{ji} + \hat{\mathbf{v}}_i(\mathbf{K}\boldsymbol{\varphi}_i - \lambda_i \mathbf{M}\boldsymbol{\varphi}_i) + \hat{\alpha}_i\left(\boldsymbol{\varphi}_i^T \mathbf{M}\boldsymbol{\varphi}_i - 1\right) \tag{14}$$

As a result, the initial sensitivity formulation of MSE is given by:

$$\frac{dMSE_{ij}^*}{dp_j} = \frac{1}{2}\boldsymbol{\varphi}_i^T \frac{\partial \mathbf{k}_j}{\partial p_j}\boldsymbol{\varphi}_i + \hat{\mathbf{v}}_i^T\left(\frac{\partial \mathbf{K}}{\partial p_j} - \lambda_i \frac{\partial \mathbf{M}}{\partial p_j}\right)\boldsymbol{\varphi}_i + \hat{\alpha}_i \boldsymbol{\varphi}_i^T \frac{\partial \mathbf{M}}{\partial p_j}\boldsymbol{\varphi}_i \tag{15}$$

where $\hat{\mathbf{v}}$ and $\hat{\alpha}$ are the multipliers of Lagrange function (L^*). These unknown multipliers were calculated by considering the first necessary condition of the Lagrange optimization problem, Eq. (12), through solving the following linear matrix system.

$$\begin{bmatrix} \mathbf{K} - \lambda_i \mathbf{M} & \vartheta \mathbf{M}\boldsymbol{\varphi}_i \\ \vartheta \boldsymbol{\varphi}_i^T \mathbf{M} & \mathbf{0} \end{bmatrix} \begin{bmatrix} \hat{\mathbf{v}} \\ 2\vartheta^{-1}\hat{\alpha} \end{bmatrix} = \begin{bmatrix} -\mathbf{k}_j \boldsymbol{\varphi}_i \\ 0 \end{bmatrix} \tag{16}$$

In this equation, ϑ is a non-zero constant used for reducing the large condition number of the sensitivity matrix. This constant is obtained by finding the largest absolute element matrix $\mathbf{K}$-$\lambda_i\mathbf{M}$ and dividing the largest absolute element of $\boldsymbol{\varphi}_i^T\mathbf{M}$.

3.3. The improved sensitivity function

Despite appropriate innovations in the initial sensitivity function of MSE, there is a great limitation to use this function in the damage detection problem. This limitation or shortcoming pertains to the lack of using the stiffness orthogonality condition as a constraint in the Lagrange function. As stated earlier, the selection of adequate constraints play prominent roles in the acceptable solution. In many optimization problems, the variables cannot be chosen arbitrarily; rather, they have to satisfy certain constraints [31]. The variables in Eq. (14) involve the design variable (p), eigenvalue (λ), and eigenvector ($\boldsymbol{\varphi}$). For the damage detection problem, the design variable alters the damage parameter or damage variable. In most real applications, structural damage is generally concerned with the adverse changes in stiffness matrix, while the mass matrix normally remains unchanged. This means that the damage parameter is directly related to structural stiffness. Therefore, the adequate constraints used in the Lagrange function should be pertinent to the stiffness matrix, which include the eigenvalue problem and stiffness orthogonality condition. Furthermore, the main premise of establishing the sensitivity function of MSE is to apply the mass-normalized mode shapes. Based on the fundamental principles of modal analysis, the mode shape of the structure is usually scaled by the mass orthogonality condition. Hence, this condition should be defined in the Lagrange optimization problem as the other constraint.

In this section, an improved sensitivity function of MSE by the Lagrange multipliers method is proposed to cope with the main limitation of the initial sensitivity of MSE. Similarly, the Lagrange function of improved formulation contains the element MSE as the objective function, while the eigenvalue problem and both orthogonality conditions are chosen as the constraints. Thus, the development of Lagrange function is expressed as follows:

$$L(\boldsymbol{p}, \lambda_i, \boldsymbol{\varphi}_i, \mathbf{v}_i, \boldsymbol{u}_i, \boldsymbol{w}_i) = MSE_{ij} + \mathbf{v}_i^T(\mathbf{K} - \lambda_i \mathbf{M})\boldsymbol{\varphi}_i + \boldsymbol{u}_i\left(\boldsymbol{\varphi}_i^T \mathbf{K}\boldsymbol{\varphi}_i - \lambda_i\right) + \boldsymbol{w}_i\left(\boldsymbol{\varphi}_i^T \mathbf{M}\boldsymbol{\varphi}_i - 1\right) \tag{17}$$

where $\mathbf{v}$, u, and w are the unknown Lagrange multipliers, which should be determined. The multiplier $\mathbf{v}$ is a vector with the same dimension as the mode shape vector. Furthermore, u and w are calculated as scalar quantities. By adding the stiffness orthogonality condition to the initial Lagrange function, it is not possible to calculate the unknown multipliers of the developed Lagrange function by the linear matrix system presented in Eq. (16). Based on the necessary conditions of Lagrange optimization problem, Eqs. (12) and (13), these multipliers are computed by taking the first-order derivative of the Lagrange function with respect to the independent variables ($\partial L/\partial \boldsymbol{\varphi}_i$ and $\partial L/\partial \lambda_i$) and multipliers ($\partial L/\partial \mathbf{v}_i$, $\partial L/\partial u_i$ and $\partial L/\partial w_i$). The partial derivative of Lagrange function with respect to the ith mode shape is given by:

$$\frac{\partial L}{\partial \boldsymbol{\varphi}_i} = \frac{\partial MSE_i}{\partial \boldsymbol{\varphi}_i} + \mathbf{v}_i^T(\mathbf{K} - \lambda_i\mathbf{M}) + \boldsymbol{u}_i\left(\left(\frac{\partial \boldsymbol{\varphi}_i}{\partial \boldsymbol{\varphi}_i}\right)^T \mathbf{K}\boldsymbol{\varphi}_i + \boldsymbol{\varphi}_i^T\mathbf{K}\left(\frac{\partial \boldsymbol{\varphi}_i}{\partial \boldsymbol{\varphi}_i}\right)\right)$$
$$+\boldsymbol{w}_i\left(\left(\frac{\partial \boldsymbol{\varphi}_i}{\partial \boldsymbol{\varphi}_i}\right)^T \mathbf{M}\boldsymbol{\varphi}_i + \boldsymbol{\varphi}_i^T\mathbf{M}\left(\frac{\partial \boldsymbol{\varphi}_i}{\partial \boldsymbol{\varphi}_i}\right)\right) = 0 \tag{18}$$

in which

$$\frac{\partial MSE_i}{\partial \boldsymbol{\varphi}_i} = \frac{1}{2}\left(\left(\frac{\partial \boldsymbol{\varphi}_i}{\partial \boldsymbol{\varphi}_i}\right)^T \mathbf{K}\boldsymbol{\varphi}_i + \boldsymbol{\varphi}_i^T\mathbf{K}\left(\frac{\partial \boldsymbol{\varphi}_i}{\partial \boldsymbol{\varphi}_i}\right)\right) = \frac{1}{2}\left(\mathbf{K}\boldsymbol{\varphi}_i + \boldsymbol{\varphi}_i^T\mathbf{K}\right) \tag{19}$$

The mass and stiffness matrices of the structure are symmetric; therefore, it is reasonable to state that $\mathbf{M}\boldsymbol{\varphi}_i = \boldsymbol{\varphi}_i^T\mathbf{M}$ and $\mathbf{K}\boldsymbol{\varphi}_i = \boldsymbol{\varphi}_i^T\mathbf{K}$. Accordingly, Eq. (18) is modified as follows:

$$\frac{\partial L}{\partial \boldsymbol{\varphi}_i} = \mathbf{K}\boldsymbol{\varphi}_i + (\mathbf{K} - \lambda_i\mathbf{M})\mathbf{v}_i + 2\boldsymbol{u}_i(\mathbf{K}\boldsymbol{\varphi}_i) + 2\boldsymbol{w}_i(\mathbf{M}\boldsymbol{\varphi}_i) = 0 \tag{20}$$

The first-order derivative of Lagrange function in relation to the eigenvalue is obtained from:

$$\frac{\partial L}{\partial \lambda_i} = -\mathbf{v}_i^T\mathbf{M}\boldsymbol{\varphi}_i - \boldsymbol{u}_i = 0 \tag{21}$$

Taking the derivatives of Lagrange function with respect to the multipliers leads to the following equations:

$$\frac{\partial L}{\partial \mathbf{v}_i} = (\mathbf{K} - \lambda_i\mathbf{M})\boldsymbol{\varphi}_i = 0 \tag{22}$$

$$\frac{\partial L}{\partial \boldsymbol{u}_i} = \boldsymbol{\varphi}_i^T\mathbf{K}\boldsymbol{\varphi}_i - \lambda_i = 0 \tag{23}$$

$$\frac{\partial L}{\partial \boldsymbol{w}_i} = \boldsymbol{\varphi}_i^T\mathbf{M}\boldsymbol{\varphi}_i - 1 = 0 \tag{24}$$

To calculate the Lagrange multipliers, $\boldsymbol{\varphi}_i^T$ is multiplied to Eq. (20). The result is:

$$\boldsymbol{\varphi}_i^T\mathbf{K}\boldsymbol{\varphi}_i + \boldsymbol{\varphi}_i^T(\mathbf{K} - \lambda_i\mathbf{M})\mathbf{v}_i + 2\boldsymbol{u}_i\left(\boldsymbol{\varphi}_i^T\mathbf{K}\boldsymbol{\varphi}_i\right) + 2\boldsymbol{w}_i\left(\boldsymbol{\varphi}_i^T\mathbf{M}\boldsymbol{\varphi}_i\right) = 0 \tag{25}$$

According to Eqs. (23) and (24), the third and fourth terms of Eq. (25) are identical to λ_i and one, respectively. Moreover, Eq. (22) obviously represents that $(\mathbf{K}\text{-}\lambda_i\mathbf{M})\boldsymbol{\phi}_i$ or $\boldsymbol{\phi}_i^T(\mathbf{K}\text{-}\lambda_i\mathbf{M})$ are always equal to zero. Therefore, the multiplier w is formulated as:

$$\boldsymbol{w}_i = -\frac{(1 + 2\boldsymbol{u}_i)}{2}\lambda_i \tag{26}$$

By inserting Eq. (26) into Eq. (20), it can be written:

$$(\mathbf{K} - \lambda_i\mathbf{M})\boldsymbol{\varphi}_i + (\mathbf{K} - \lambda_i\mathbf{M})\mathbf{v}_i + 2\boldsymbol{u}_i(\mathbf{K} - \lambda_i\mathbf{M})\boldsymbol{\varphi}_i = 0 \tag{27}$$

With regard to Eq. (22), the first and third expressions of Eq. (27) are given by zero. Hence, the multiplier $\mathbf{v}$ is determined by solving the following equation:

$$(\mathbf{K} - \lambda_i\mathbf{M})\mathbf{v}_i = 0 \tag{28}$$

Having the vector $\mathbf{v}$, the other scalar multiplier u is calculated through Eq. (21) as:

$$\boldsymbol{u}_i = -\mathbf{v}_i^T\mathbf{M}\boldsymbol{\varphi}_i \tag{29}$$

Eventually, the scalar multiplier w is gained by inserting the amount of multiplier u into Eq. (26). Once the multipliers of Lagrange function have been obtained, the total derivative of Lagrange function with respect to the damage parameter p in jth element is taken as:

$$\frac{dL}{d\boldsymbol{p}_j} = \frac{dMSE_{ij}}{d\boldsymbol{p}_j} + \frac{d\left(\mathbf{B}_{\mathbf{P}}\beta_{\mathbf{L}}\right)}{d\boldsymbol{p}_j} \tag{30}$$

For the sake of simplicity, $\mathbf{B_P}$ and $\boldsymbol{\beta}_\mathbf{L}$ are:

$$\mathbf{B_P} = \left[(\mathbf{K} - \lambda_i \mathbf{M})\boldsymbol{\varphi}_i \quad \boldsymbol{\varphi}_i^T \mathbf{K} \boldsymbol{\varphi}_i - \lambda_i \quad \boldsymbol{\varphi}_i^T \mathbf{M} \boldsymbol{\varphi}_i - 1 \right] \tag{31}$$

$$\beta_\mathbf{L} = \left[\mathbf{v}^T \quad \boldsymbol{u} \quad \boldsymbol{w} \right]^T \tag{32}$$

Developing the derivatives of $\mathbf{B_P}$ and $\boldsymbol{\beta}_\mathbf{L}$ with respect to the damage parameter p_j, one can obtain:

$$\frac{d\left(\mathbf{B_P}\beta_\mathbf{L}\right)}{d\boldsymbol{p}_j} = \frac{d\mathbf{B_P}}{d\boldsymbol{p}_j}\beta_\mathbf{L} + \mathbf{B_P}\frac{d\beta_\mathbf{L}}{d\boldsymbol{p}_j} \tag{33}$$

Based on the second necessary condition of the Lagrange optimization problem presented in Eq. (13), one can realize that the constraints of Lagrange function always correspond to zero. On the other hand, $\mathbf{B_P}$ is equivalent to $G(x_1,x_2,\ldots,x_{nv})$ in the original Lagrange optimization problem. Therefore, it can be argued that $\mathbf{B_P}$ is also identical to zero. Accordingly, the second term of Eq. (33) is eliminated and this equation can be rewritten as follows:

$$\frac{d\left(\mathbf{B_P}\beta_\mathbf{L}\right)}{d\boldsymbol{p}_j} = \frac{d\mathbf{B_P}}{d\boldsymbol{p}_j}\beta_\mathbf{L} \tag{34}$$

According to the theory of variational principle [33,34], the following equations are always valid:

$$(\mathbf{B_P})^T \beta_\mathbf{L} = 0 \tag{35}$$

$$\left(\mathbf{B_P} + \frac{d\mathbf{B_P}}{dp_j}\right)^T \beta_\mathbf{L} = 0 \tag{36}$$

Since $\mathbf{B_P}$ corresponds to zero, it is apparent from Eq. (35) that $\boldsymbol{\beta}_\mathbf{L}$ is always non-zero. Based on Eq. (36), where $\mathbf{B_P}=0$ and $\boldsymbol{\beta}_\mathbf{L}\neq 0$, one can deduce that the total derivative of $\mathbf{B_P}$ with respect to the damage parameter ($d\mathbf{B_P}/dp_j$) is identical to zero, which means that $d(\mathbf{B_P}\,\boldsymbol{\beta}_\mathbf{L})/dp_j = 0$. Under such circumstances, the total derivative of Lagrange function corresponds to the total derivative of MSE ($dL/dp_j = dMSE_{ij}/dp_j$). On the other hand, the total derivative of Lagrange function can be written based on the partial derivative as:

$$\frac{\partial L}{\partial \boldsymbol{p}_j} + \frac{\partial L}{\partial \boldsymbol{\varphi}_i}\frac{d\boldsymbol{\varphi}_i}{d\boldsymbol{p}_j} + \frac{\partial L}{\partial \lambda_i}\frac{d\lambda_i}{d\boldsymbol{p}_j} = \frac{\partial MSE}{\partial \boldsymbol{p}_j} + \frac{\partial \mathbf{B_P}}{\partial \boldsymbol{p}_j}\beta_\mathbf{L} \tag{37}$$

Based on the first necessary condition of Lagrange optimization problem, the partial derivatives of Lagrange function with respect to the eigenvalue and eigenvector are identical to zero. This means that the second and third terms of the left-hand side of Eq. (37) become zero. Therefore:

$$\frac{dL}{d\boldsymbol{p}_j} = \frac{\partial L}{\partial \boldsymbol{p}_j} \tag{38}$$

$$\frac{dL}{d\boldsymbol{p}_j} = \frac{\partial MSE_{ij}}{\partial \boldsymbol{p}_j} + \frac{\partial \mathbf{B_P}}{\partial \boldsymbol{p}_j}\beta_\mathbf{L} \tag{39}$$

Note that the partial derivative of $\mathbf{B_P}\boldsymbol{\beta}_\mathbf{L}$ with respect to p_j is non-zero. In other words, Eqs. (35) and (36) are only valid for the total derivative of $\mathbf{B_P}\boldsymbol{\beta}_\mathbf{L}$. On this basis, the partial derivative of $\mathbf{B_P}$ with respect to the damage parameter is given by:

$$\frac{\partial \mathbf{B_P}}{\partial \boldsymbol{p}_j} = \left[\left(\frac{\partial \mathbf{K}}{\partial \boldsymbol{p}_j} - \lambda_i \frac{\partial \mathbf{M}}{\partial \boldsymbol{p}_j} \right)\boldsymbol{\varphi}_i \quad \boldsymbol{\varphi}_i^T \frac{\partial \mathbf{K}}{\partial \boldsymbol{p}_j}\boldsymbol{\varphi}_i \quad \boldsymbol{\varphi}_i^T \frac{\partial \mathbf{M}}{\partial \boldsymbol{p}_j}\boldsymbol{\varphi}_i \right] \tag{40}$$

Eventually, based on the results of Eqs. (38)–(40) one can write:

$$\frac{dMSE_{ij}}{d\boldsymbol{p}_j} = \frac{\partial MSE_{ij}}{\partial \boldsymbol{p}_j} + \frac{\partial \mathbf{B_P}}{\partial \boldsymbol{p}_j}\beta_\mathbf{L} \tag{41}$$

This equation represents that the total derivative of element MSE is equivalent to the partial derivatives of Lagrange function and its constraints. By inserting Eq. (40) and $\boldsymbol{\beta}_\mathbf{L}$ into Eq. (41), the improved sensitivity function of MSE is proposed as:

$$\frac{dMSE_{ij}}{d\boldsymbol{p}_j} = \frac{1}{2}\boldsymbol{\varphi}_i^T \frac{\partial \mathbf{k}_j}{\partial \boldsymbol{p}_j}\boldsymbol{\varphi}_i + (\mathbf{v}_i + \boldsymbol{u}_i\boldsymbol{\varphi}_i)^T \frac{\partial \mathbf{K}}{\partial \boldsymbol{p}_j}\boldsymbol{\varphi}_i + \left(w_i\boldsymbol{\varphi}_i - \lambda_i \mathbf{v}_i\right)^T \frac{\partial \mathbf{M}}{\partial \boldsymbol{p}_j}\boldsymbol{\varphi}_i \tag{42}$$

By neglecting the first-order derivative of the mass matrix with respect to the damage parameter, the improved sensitivity function of MSE for the process of damage detection is presented as:

$$\frac{dMSE_{ij}}{d\boldsymbol{p}_j} = \frac{1}{2}\boldsymbol{\varphi}_i^T\frac{\partial \mathbf{k}_j}{\partial \boldsymbol{p}_j}\boldsymbol{\varphi}_i + (\mathbf{v}_i + \boldsymbol{u}_i\boldsymbol{\varphi}_i)^T\frac{\partial \mathbf{K}}{\partial \boldsymbol{p}_j}\boldsymbol{\varphi}_i \tag{43}$$

where $\partial\mathbf{K}/\partial p_j$ in the partial derivative of the global stiffness matrix with respect to the damage parameter, which can obtained as follows [26]:

$$\frac{\partial \mathbf{K}}{\partial \boldsymbol{p}_j} = \sum_{t=1}^{\boldsymbol{ne}}\frac{\partial \mathbf{k}_t}{\partial \boldsymbol{p}_j}, \qquad j = 1, 2, \ldots, \boldsymbol{ne} \tag{44}$$

It should be noted that the first-order derivatives of the local and global stiffness matrices with respect to the damage parameter are typically determined by the well-known finite difference methods. Based on the forward difference method used in this study, Eq. (44) is rewritten as:

$$\frac{\partial \mathbf{K}}{\partial \boldsymbol{p}_j} = \sum_{t=1}^{\mathbf{ne}}\frac{\mathbf{k}_t\left(\boldsymbol{p}_j + \Delta\boldsymbol{p}_j\right) - \mathbf{k}_t\left(\boldsymbol{p}_j\right)}{\Delta\boldsymbol{p}_j}, \qquad j = 1, 2, \ldots, \boldsymbol{ne} \tag{45}$$

The key benefit of the improved sensitivity of MSE compared with Eq. (10) is to avoid using the derivative of mode shape in the establishment of sensitivity formulation. The comparison of the initial and improved sensitivity functions of MSE indicates that the major differences between these formulations are pertinent to the number of constraints used in the Lagrange function, the distinct ways of calculating the Lagrange multipliers, and the direct consistency of improved sensitivity function to damage detection problems.

4. Damage detection problem

Damage detection is a comparative process between two different phases of a structure, including the undamaged and damaged conditions. Due to the major development of numerical modeling for structural systems through powerful engineering software and the availability of mechanical characteristics of FE models, most of the vibration-based damage detection methods are based on model updating strategy [8,18,20,35,36]. On this basis, it is assumed that the FE or analytical model of the real structure represents the undamaged structural condition, whereas the experimental or tested structure implies the damaged state. For the undamaged structure, the inherent structural properties and analytical modal parameters are simply obtained from the FE model. In contrast, the only experimental modal parameters are available in the tested structure. The main premise behind the damage detection problem based on model updating strategy is to update or calibrate the FE model of the undamaged structure by model updating techniques before the implementation of damage detection process [18].

Because model updating is an inverse problem and the relationship between structural parameters and measured responses is inherently nonlinear, sensitivity-based methods are developed to simplify solving this problem using linearization of equations [9]. In other words, the sensitivity function linearly describes a relationship between the residual of measured responses between the undamaged and damaged states as well as changes in structural parameters. The linear inverse problem, on the other hand, involves a residual vector, a sensitivity or coefficient matrix, and an unknown vector that should be determined. For the process of damage detection, a damage equation by means of the linear inverse problem is defined as follows:

$$\mathbf{S}\cdot\mathbf{a} = \mathbf{r} \tag{46}$$

where $\mathbf{S} \in \mathfrak{R}^{m\times ne}$ is the sensitivity matrix, where m and ne are representative of the number of measured modes, and the number of elements. In addition, $\mathbf{r} \in \mathfrak{R}^{m}$ denotes the residual vector including the discrepancy of measurable outputs (i.e. incomplete modal parameters) in the undamaged and damaged conditions, and $\mathbf{a} \in \mathfrak{R}^{ne}$ represents the unknown damage vector. A significant note is that the residual is a function of sensitivity matrix. For example, the residual for the sensitivity of mode shape or natural frequency is the discrepancy of mode shapes or modal frequencies in the undamaged and damaged states. Therefore, the compatible residual with the sensitivity of MSE can be expressed as:

$$\mathbf{r}_i = \mathbf{MSE}_{ij}^{d} - \mathbf{MSE}_{ij}^{u} \tag{47}$$

In this equation, the subscriptions d and u represent the damaged and undamaged conditions of the structure, respectively. Since the stiffness matrix of the damaged structure is not available, the residual of element MSE in the i^{th} measured mode can be rewritten in the following form:

$$\mathbf{r}_i = \frac{1}{2}\sum_{j=1}^{\boldsymbol{ne}}\Delta\boldsymbol{\varphi}_i^T\mathbf{k}_j\Delta\boldsymbol{\varphi}_i \tag{48}$$

in which

$$\Delta \boldsymbol{\varphi}_i = \hat{\boldsymbol{\varphi}}_i - \boldsymbol{\varphi}_i \tag{49}$$

It is important to point out that $\hat{\boldsymbol{\varphi}}_i$ denotes the i^{th} measured mode shape of the tested structure in the damaged state. Because the measured modal parameters are incomplete, the sensitivity matrix is usually generated as a rectangular matrix. Additionally, it is possible that some singular values of the inverse of this matrix are close to zero, which means that the rectangular sensitivity matrix becomes sparse and ill-conditioned. Although the least-squares method is a well-known mathematical technique for solving the damage equation, the use of inverse operation for the rectangular, sparse, and ill-conditioned sensitivity matrix leads to an unrealistic and erroneous solution. Moreover, small perturbations in the modal data caused by noise may result in poor damage detection results. Under such circumstances, the damage equation is an ill-posed problem and regularization methods need to solve this problem by filtering out the influence of noise on the measured modal data [17]. In this article, an iterative regularization method (RLSMR) based on Krylov subspace is introduced to solve the ill-posed damage equation with the special focus on using the sparse and ill-conditioned sensitivity matrix.

5. Regularized solution of ill-posed damage equation

5.1. Tikhonov regularization method

The most comment way for the regularized solution of ill-posed damage detection equation is to use Tikhonov regularization method. In this method, the solution of Eq. (46) is performed as the minimization of the following objective function:

$$\mathbf{J}(\mathbf{a}) = \|\mathbf{S}\mathbf{a} - \mathbf{r}\|_2^2 + \gamma^2\|\mathbf{a}\|_2^2 \tag{50}$$

where the regularization parameter $\gamma \geq 0$ controls the weight given to the solution $\|\mathbf{a}\|_2^2$ relative to the residual norm $\|\mathbf{S}\mathbf{a} - \mathbf{r}\|_2^2$. When the sensitivity matrix is ill-conditioned and rectangular, the classical solution of Eq. (50) through pseudo-inverse operation does not make realistic and stable results. One way to circumvent this drawback is to decompose the sensitivity matrix by singular value decomposition (SVD) technique. Therefore, one can write:

$$\mathbf{S} = \bar{\mathbf{U}}\boldsymbol{\Sigma}\bar{\mathbf{V}}^T = \sum_{i=1}^{m} \bar{\boldsymbol{\sigma}}_i \bar{\boldsymbol{u}}_i \bar{\mathbf{v}}_i^T \tag{51}$$

where $\bar{\mathbf{U}}=[\bar{\boldsymbol{u}}_1 \ldots \bar{\boldsymbol{u}}_m] \in \Re^{m\times m}$ and $\bar{\mathbf{V}}=[\bar{\mathbf{v}}_1 \ldots \bar{\mathbf{v}}_m] \in \Re^{n_e\times m}$. In this equation, the diagonal matrix $\boldsymbol{\Sigma}=[\bar{\sigma}_1 \ldots \bar{\sigma}_m] \in \Re^{m\times m}$ consists of m singular values in descending order. On this basis, the regularized solution of the damage equation by Tikhonov regularization method is given by:

$$\mathbf{a} = \sum_{i=1}^{m} \mathbf{f}_i(\gamma) \frac{\bar{\boldsymbol{u}}_i^T \mathbf{r}}{\bar{\boldsymbol{\sigma}}_i} \bar{\mathbf{v}}_i \tag{52}$$

In Eq. (52), the expression $f_i(\gamma) = \left(\bar{\sigma}_i^2/\bar{\sigma}_i^2 + \gamma^2\right)$ is called filter factor. It is apparent that the use of filter factor in the regularized solution of the damage equation damps the effects associated with the small singular values and ill-conditioning of sensitivity matrix. In other words, $\gamma=0$ causes an un-regularized solution, where the filter factors are unite for all singular values.

5.2. Regularized least squares minimal residual method

The RLSMR method is a development of Least Squares Minimal Residual (LSMR) technique for a regularized solution of the sparse inverse problem $\mathbf{S}\mathbf{a}=\mathbf{r}$ and the sparse least squares problem $\min\|\mathbf{S}\mathbf{a}\text{-}\mathbf{r}\|_2$. Both methods exploit iterative and bidiagonalization algorithms based on Krylov subspace for the solution of sparse linear systems. The LSMR method is analytically equivalent to Minimal Residual (MINRES) technique applied to the normal equation $\mathbf{S}^T\mathbf{S}\mathbf{a}_k = \mathbf{S}^T\mathbf{r}$ in such a way that quantities $\|\mathbf{S}^T\mathbf{e}_k\|_2$ are monotonically decreasing, In this approach, $\mathbf{e}_k=\mathbf{r}-\mathbf{S}\mathbf{a}_k$ represents the residual of problem for the current iteration $\mathbf{a}_k$. The LSMR method in fact attempts to obtain $\mathbf{a}_k$ in the k^{th} iteration as an approximate solution of the damage equation through the l_2-minimization of $\mathbf{S}^T\mathbf{e}_k$ [37].

Most of the Krylov subspace iterative methods require square sensitivity matrix for the solution of sparse inverse problem. When the modal parameters are incomplete, the sensitivity matrix becomes rectangular; therefore, the majority of iterative methods may be useless. Among the Krylov subspace iterative methods, the LSMR method is capable of solving linear systems with rectangular and sparse sensitivity matrix [38]. Nonetheless, this technique is not a proper choice for solving the damage equation when noise contaminates the modal parameters. To overcome this drawback, the RLSMR method solves the sparse inverse problem in an iterative manner by adding a regularization parameter to the algorithm of LSMR method.

In a similar way, the RLSMR method utilizes the bidiagonalization algorithm proposed by Golub and Kahan [39]. This algorithm transforms or reduces the sensitivity matrix and residual vector to upper-bidiagonal form in the following equations:

$$\beta_1 \mathbf{x}_1 = \mathbf{r} \tag{53}$$

$$\alpha_1 \mathbf{y}_1 = \mathbf{S}^T \mathbf{x}_1 \tag{54}$$

Initially, the quantity β_1 are defined as the square l_2-norm of the vector $\mathbf{r}$. As such, the unknown vector $\mathbf{x}_1$ is described as follows:

$$\mathbf{x}_1 = \frac{\mathbf{r}}{\beta_1} = \frac{\mathbf{r}}{\|\mathbf{r}\|_2^2} \tag{55}$$

The scalar amount α_1 is then obtained from the square l_2-norm of $\mathbf{S}^T\mathbf{x}_1$, after calculating the vector $\mathbf{x}_1$. Eventually, the unknown vector $\mathbf{y}_1$ is expressed as:

$$\mathbf{y}_1 = \frac{\mathbf{S}^T \mathbf{x}_1}{\alpha_1} = \frac{\mathbf{S}^T \mathbf{x}_1}{\left\| \mathbf{S}^T \mathbf{x}_1 \right\|_2^2} \tag{56}$$

For k = 1,2,…, Eqs. (53) and (54) should be written as:

$$\beta_{k+1} \mathbf{x}_{k+1} = \mathbf{S}\mathbf{y}_k - \alpha_k \mathbf{x}_k \tag{57}$$

$$\alpha_{k+1} \mathbf{y}_{k+1} = \mathbf{S}^T \mathbf{x}_{k+1} - \beta_{k+1} \mathbf{y}_k \tag{58}$$

In these equations, for k = 1, the vectors $\mathbf{x}_1$ and $\mathbf{y}_1$ are calculated by Eqs. (55) and (56), respectively. Furthermore, the unknown parameters including α, β, $\mathbf{x}$ and $\mathbf{y}$ in the $(k+1)^{th}$ iteration are computed in a similar way with the first iteration. For a more clarification, the scalar parameters β and α in the $(k+1)^{th}$ iteration are formulated as the square l^2-norm of $\mathbf{S}\mathbf{y}_k - \alpha_k \mathbf{x}_k$ and $\mathbf{S}^T\mathbf{x}_{k+1} - \beta_{k+1}\mathbf{y}_k$, respectively. Moreover, the vectors $\mathbf{x}_{k+1}$ and $\mathbf{y}_{k+1}$ are expressed as:

$$\mathbf{x}_{k+1} = \frac{\mathbf{S}\mathbf{y}_k - \alpha_k \mathbf{x}_k}{\beta_{k+1}} = \frac{\mathbf{S}\mathbf{y}_k - \alpha_k \mathbf{x}_k}{\left\| \mathbf{S}\mathbf{y}_k - \alpha_k \mathbf{x}_k \right\|_2^2} \tag{59}$$

$$\mathbf{y}_{k+1} = \frac{\mathbf{S}^T \mathbf{x}_{k+1} - \beta_{k+1} \mathbf{y}_k}{\alpha_{k+1}} = \frac{\mathbf{S}^T \mathbf{x}_{k+1} - \beta_{k+1} \mathbf{y}_k}{\left\| \mathbf{S}^T \mathbf{x}_{k+1} - \beta_{k+1} \mathbf{y}_k \right\|_2^2} \tag{60}$$

At each iteration, the scalars $\beta \geq 0$ and $\alpha \geq 0$ are chosen such that $\|\mathbf{x}\|_2 = \|\mathbf{y}\|_2 = 1$. After k iteration, an upper-bidiagonal matrix $\mathbf{B}_k$ and two matrices including $\mathbf{X}_k = [\mathbf{x}_1 \ \ldots \ \mathbf{x}_k]$ and $\mathbf{Y}_k = [\mathbf{y}_1 \ \ldots \ \mathbf{y}_k]$ from the vectors $\mathbf{x}$ and $\mathbf{y}$ can be constructed. The upper-bidiagonal matrix $\mathbf{B}_k$ is established as follows:

$$\mathbf{B}_k = \begin{bmatrix} \alpha_1 & & & \\ \beta_1 & \alpha_2 & & \\ & \beta_2 & \ddots & \\ & \ddots & \ddots & \alpha_k \\ & & & \beta_{k+1} \end{bmatrix} \tag{61}$$

The recurrence of Eqs. (53), (54), (57), and (58) may be written as:

$$\begin{aligned} &\mathbf{X}_{k+1}(\beta_1 \mathbf{z}_1) = \mathbf{r}, \\ &\mathbf{S}\mathbf{Y}_k = \mathbf{X}_{k+1}\mathbf{B}_k, \\ &\mathbf{S}^T \mathbf{X}_{k+1} = \mathbf{Y}_k \mathbf{B}_k^T + \alpha_{k+1} \mathbf{y}_{k+1} \mathbf{z}_{k+1}^T \end{aligned} \tag{62}$$

where $\mathbf{z}_1$ and $\mathbf{z}_{k+1}$ are the first and last columns of the identity matrix $\mathbf{I}$, respectively. The solution of ill-posed damage equation by the RLSMR method is similar to the LSMR method with the exception of adding a regularization term to minimize $\left\| \hat{\mathbf{S}}\mathbf{a} - \hat{\mathbf{r}} \right\|_2$, where $\hat{\mathbf{S}} = [\mathbf{S} \ \ \gamma\mathbf{I}]^T$, $\hat{\mathbf{r}} = [\mathbf{r} \ \ \boldsymbol{0}]^T$ and $\hat{\mathbf{e}} = \hat{\mathbf{r}} - \hat{\mathbf{S}}\mathbf{a}$ represents the residual of minimization problem based on the RLSMR method. By defining these expressions and applying the bidiagonalization process, the algorithm of RLSMR method is presented in Table 1.

Once the parameters of RLSMR algorithm have been calculated, the regularized solution of damage equation is carried out to obtain the damage vector ($\mathbf{a}_k$) in the following form:

$$\mathbf{a}_k = \mathbf{a}_{k-1} + \left(\frac{\xi_k}{\rho_k \cdot \bar{\rho}_k} \right) \bar{\mathbf{h}}_k \tag{63}$$

Table 1
The algorithm of RLSMR method [37].

Step 1: Initialize

$$\beta_1\mathbf{x}_1=\mathbf{r},\quad \alpha_1\mathbf{y}_1=\mathbf{S}^T\mathbf{x}_1,\quad \bar{\alpha}_1=\alpha_1,\quad \bar{\xi}_1=\alpha_1\beta_1,\quad \rho_0=1,\quad \bar{\rho}_0=1$$
$$\bar{c}_0=1,\quad \bar{f}_0=1,\quad \ddot{\beta}_1=\beta_1,\quad \dot{\beta}_0=0,\quad \dot{\rho}_0=0,\quad \tau_{-1}=0,$$
$$\bar{\theta}_0=0,\quad \xi_0=0,\quad d_0=0,\quad \mathbf{h}_1=\mathbf{y}_1,\quad \bar{\mathbf{h}}_0=0,\quad x_0=0.$$

Step 2: For k=1,2,…, repeat steps 3–12 as follows

Step 3: Continue the bidiagonalization

$$\beta_{k+1}\mathbf{x}_{k+1}=\mathbf{S}\mathbf{y}_k-\alpha_k\mathbf{x}_k,\quad \alpha_{k+1}\mathbf{y}_{k+1}=\mathbf{S}^T\mathbf{x}_{k+1}-\beta_{k+1}\mathbf{y}_k$$

Step 4:

$$\hat{\alpha}_k=\sqrt{\left(\bar{\alpha}_k^2+\boldsymbol{\gamma}^2\right)},\qquad \hat{c}_k=\bar{\alpha}_k/\hat{\alpha}_k,\qquad \hat{f}_k=\boldsymbol{\gamma}/\hat{\alpha}_k.$$

Step 5:

$$\rho_k=\sqrt{\left(\hat{\alpha}_k^2+\beta_{k+1}^2\right)},\quad \hat{c}_k=\hat{\alpha}_k/\rho_k,\quad f_k=\beta_{k+1}/\rho_k,\quad \theta_{k+1}=f_k\alpha_{k+1},\quad \bar{\alpha}_{k+1}=c_k\alpha_{k+1}.$$

Step 6:

$$\bar{\theta}_k=\bar{f}_{k-1}\rho_k,\qquad \bar{\rho}_k=\sqrt{\left(\bar{c}_{k-1}\rho_k\right)^2+\theta_{k+1}^2},\qquad \bar{c}_k=\bar{c}_{k-1}\rho_k/\bar{\rho}_k,$$
$$\bar{f}_k=\theta_{k+1}/\bar{\rho}_k,\qquad \xi_k=\bar{c}_k\bar{\xi}_k,\qquad \bar{\xi}_{k+1}=-\bar{f}_k\bar{\xi}_k.$$

Step 7: Update $\mathbf{h}$, $\bar{\mathbf{h}}$ and $\mathbf{a}$

$$\bar{\mathbf{h}}_k=\mathbf{h}_k-\left(\frac{\bar{\theta}_k\cdot\rho_k}{\rho_{k-1}\cdot\bar{\rho}_{k-1}}\right)\bar{\mathbf{h}}_{k-1},\quad \mathbf{a}_k=\mathbf{a}_{k-1}+\left(\frac{\xi_k}{\rho_k\cdot\bar{\rho}_k}\right)\bar{\mathbf{h}}_k,\quad \mathbf{h}_{k+1}=\mathbf{y}_{k+1}-\left(\frac{\theta_{k+1}}{\rho_k}\right)\mathbf{h}_k$$

Step 8:

$$\bar{\bar{\beta}}_k=\hat{c}_k\ddot{\beta}_k,\qquad \breve{\beta}_k=-\hat{f}_k\ddot{\beta}_k,\qquad \hat{\beta}_k=c_k\bar{\bar{\beta}}_k,\qquad \ddot{\beta}_{k+1}=-\hat{f}_k\bar{\bar{\beta}}_k$$

Step 9: If k $\geq$ 2

$$\tilde{\rho}_{k-1}=\sqrt{\left(\dot{\rho}_{k-1}^2+\bar{\theta}_{k+1}^2\right)},\qquad \tilde{c}_{k-1}=\dot{\rho}_{k-1}/\tilde{\rho}_{k-1},\qquad \tilde{f}_{k-1}=\bar{\theta}_k/\tilde{\rho}_{k-1},$$
$$\tilde{\theta}_k=\tilde{f}_{k-1}\tilde{\rho}_k,\qquad \dot{\rho}_k=\tilde{c}_{k-1}\bar{\rho}_k,\qquad \tilde{\beta}_{k-1}=\tilde{c}_{k-1}\dot{\beta}_{k-1}+\tilde{f}_{k-1}\hat{\beta}_k,$$
$$\dot{\beta}_k=-\tilde{f}_{k-1}\dot{\beta}_{k-1}+\tilde{c}_{k-1}\tilde{\beta}_k.$$

Step 10: Update $\tilde{\tau}_{k-1}$ forward substitution

$$\tilde{\tau}_{k-1}=\left(\xi_{k-1}-\tilde{\theta}_{k-1}\tilde{\tau}_{k-2}\right)/\tilde{\rho}_{k-1},\qquad \tilde{\tau}_k=\left(\xi_k-\tilde{\theta}_k\tilde{\tau}_{k-1}\right)/\dot{\rho}_k,$$

Step 11: Compute $\|\hat{\mathbf{e}}_k\|$

$$d_k=d_{k-1}+\breve{\beta}_k^2,\qquad \eta=d_k+\left(\dot{\beta}_k-\dot{\tau}_k\right)^2+\ddot{\beta}_{k+1}^2,\qquad \|\hat{\mathbf{e}}_k\|=\sqrt{\eta}$$

Step 12: Compute:
$\|\hat{S}^T\hat{\mathbf{e}}_k\|$, $\|\mathbf{a}\|$, $\|\hat{S}\|$, and the condition number of $\hat{S}$.

Step 13:
Terminate iterations based on the same stopping rules as LSQR [40].

in which

$$\bar{\mathbf{h}}_k=\mathbf{h}_k-\left(\frac{\bar{\theta}_k\cdot\rho_k}{\rho_{k-1}\cdot\bar{\rho}_{k-1}}\right)\bar{\mathbf{h}}_{k-1} \tag{64}$$

$$\mathbf{h}_{k+1}=\mathbf{y}_{k+1}-\left(\frac{\theta_{k+1}}{\rho_k}\right)\mathbf{h}_k \tag{65}$$

Applying the bidiagonalization process and regularization parameter, the RLSMR method makes an iterative algorithm for the regularized solution of the ill-posed damage equation with the sparse and ill-conditioned sensitivity matrix. As a result, the RLSMR method can be a more reliable and influential solution approach in comparison with the direct regularization methods. The only remaining unknown characteristic in the algorithm of RLSMR is the regularization parameter, which will be discussed in the next section.

5.3. Determining an optimal regularization parameter

The regularized solution of the majority of ill-posed problems through direct or iterative regularization methods depends

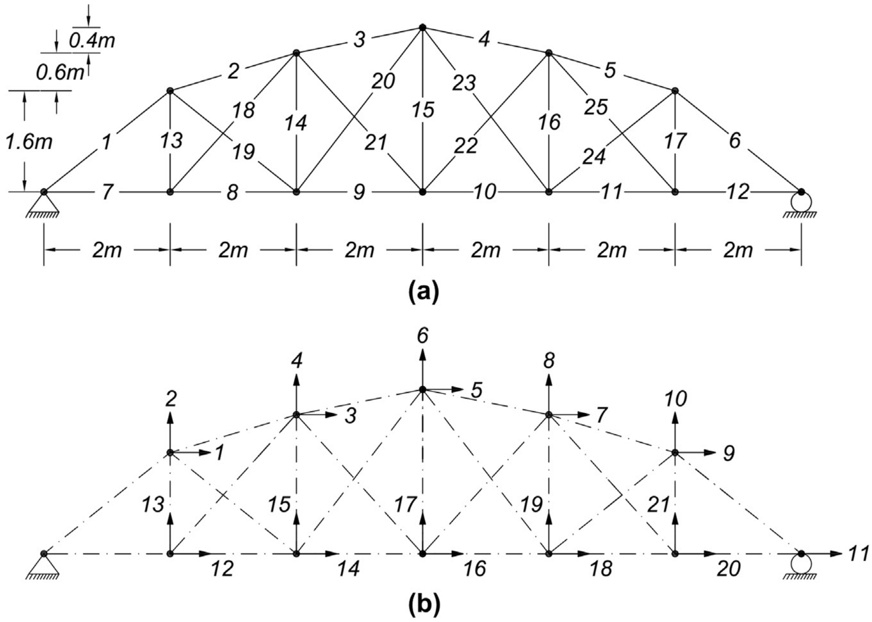

Fig. 1. The FE model of planner truss: (a) the model dimensions and elements, (b) the model DOFs.

strongly on the regularization parameter [41–43]. Finding an optimal regularization value is a crucial process, because a very small regularization quantity will not be any influence on the ill-posed problem and a very large amount results in a great deviation from the original problem [44]. The most common methods for the determination of regularization parameter are discrepancy principle, generalized cross-validation (GCV) and L-curve [43]. Choosing an appropriate method relies on the size of noise level in vibration measurements. If the size of error is known, the discrepancy principle method may be useful. In reality, the size of noise level is often unknown; thus, the optimal regularization parameter can be estimated by the GCV and L-curve methods. The GCV function for the estimation of Tikhonov regularization parameter is defined as [24]:

$$GCV(\gamma) = \frac{\boldsymbol{m}\sum_{i=1}^{\boldsymbol{m}}\left[\left(1 - \frac{\bar{\sigma}_i^2}{\bar{\sigma}_i^2+\gamma^2}\right)\bar{\mathbf{u}}_i^T\mathbf{r}\right]^2}{\left[\sum_{i=1}^{\boldsymbol{m}}\left(1 - \frac{\bar{\sigma}_i^2}{\bar{\sigma}_i^2+\gamma^2}\right)\right]^2} \tag{66}$$

However, the direct methods (i.e. discrepancy principle, L-curve, and GCV) may be impractical in the case of using Krylov subspace iterative methods or existing a large sensitivity matrix [43]. In such circumstances, projection or hybrid methods are normally suggested to determine the optimal regularization value, particularly for solving the ill-posed problems by Krylov subspace iterative methods.

Unlike the direct methods that discretize the solution of ill-posed problem onto a finite dimensional space, a projected problem projects the solution onto a k-dimensional subspace leading to a sufficient regularizing effect [43]. To put it another way, the number of iterations (k) required by the Krylov subspace iterative methods provides a regularization value. In a projection method, the type of iterative method, the number of iterations (subspaces), and the amount of stopping point for the termination of iterations are prominent issues of determining the optimal regularization parameter. However, the use of projection method alone may not provide a reliable and acceptable regularization quantity, particularly when the number of iterations or subspaces is relatively small. In order to deal with this limitation, the hybrid method is an appropriate choice. In general, this method combines a projection method and a direct regularization technique. In this article, a combination of projected GCV function with the conventional GCV function for Tikhonov regularization technique is used as a hybrid method. The idea behind using Tikhonov regularization technique is to regularize the projected problem for some iterations. Applying the filter factor of Tikhonov regularization method obtained by the singular values of the upper-bidiagonal matrix $\mathbf{B}_k$ and a regularization value (γ), the hybrid GCV function is formulated as:

$$GCV(\gamma)_{\boldsymbol{k}} = \frac{\left\|\hat{\mathbf{e}}_k\right\|_2^2}{\left(\boldsymbol{k} + 1 - \sum_{t=1}^{\boldsymbol{k}}\frac{\sigma_t^2}{\sigma_t^2+\gamma^2}\right)^2} \tag{67}$$

where σ_t is the t$^{\text{th}}$ singular value of $\mathbf{B}_k$ in descending order at the k iteration. The hybrid GCV function obviously indicates

Table 2
The invariant cross sections of the truss structure.

Element No.	Area (m^2)
1–6	0.0018
7–12	0.0015
13–17	0.0010
18–25	0.0012

Table 3
The new damage cases for the planner truss structure.

Case no.	Element no.	Stiffness reduction factor (%)
1	4	5%
	10	7.5%
2	3	5%
	9	10%
	20	12%
	25	15%

that the determination of optimal regularization value depends on the residual of RLSMR method, the number of iterations, and the bidiagonalization algorithm for the construction of upper-bidiagonal matrix. The full discussion of determining the regularization parameter by the projection and hybrid methods is beyond the scope of this article. Further comprehensive details can be found in [43,45].

6. Numerical study

In order to demonstrate the accuracy and performance of the improved and proposed methods in damage localization and quantification, a numerical model of truss structure is applied as shown in Fig. 1(a). This model is a well-known numerical structure, which has widely been used in vibration-based applications [46–48]. An analytical FE model of the truss is constructed by in-house MATLAB codes, which serves as the original or baseline model of the truss structure without damage. The FE model consists of 12 nodes, 25 bar elements, and 21 DOFs as illustrated in Fig. 1(b). It is assume that the truss elements are made from steel material with the modulus of elasticity 200 GPa, Poisson's ratio 0.3, the material density 7850 kg/m^3, and invariant cross sections given in Table 2.

For this structure, several changes in the stiffness and mass matrices have been defined to use in the FE model updating problem in order for the calibration of inherent physical properties of the truss structure. There are some important points for using these structural changes in the damage identification problem. First, it can be neglected the mass variations resulting from the lack of correlation with damage. Hence, it is plausible to assume that the mass matrix of the structure remains unchanged. Second, in most real-world structures, damage causes adverse changes as reductions in structural stiffness. Therefore, stiffness reduction factors are only applied to perform the procedures of damage localization and quantification. Third, the reduction factors used in some studies present large changes in the stiffness matrix, which it is relatively equivalent to large structural damage. An underlying issue in the damage detection problem is to seek whether damage identification methods are able to detect small damage. As a result, new damage cases are defined to assess the performance of the improved and proposed methods in detecting small damage. For this purpose, structural damage is simply simulated as reductions in axial rigidity of some elements as presented in Table 3.

The FE model with the reduced axial rigidity is then used to generate the simulated modal parameters of the tested structure. The modal data extracted from this structure serve as the measured modal parameters in the damaged condition. To simulate the incompleteness conditions of the modal data, it is assumed that the first five eigenvalues and eight modal displacements at the DOFs 2, 5, 6, 8, 13, 15, 19, and 21 are measurable. Since the mass matrix of the FE model in the undamaged state is available, the complete analytical mode shapes ($\boldsymbol{\varphi}$) are scaled by the mass orthogonality condition. Additionally, the measured incomplete modal displacements of the tested structure are normalized using Eq. (6) to provide the mass-normalized incomplete mode shapes ($\hat{\boldsymbol{\varphi}}^{m}$). Applying the SEREP transformation matrix, eventually, the normalized incomplete modal displacements are expanded to produce the complete mode shapes ($\hat{\boldsymbol{\varphi}}$) for the tested structure.

6.1. Effect of measured modes on sensitivity matrix

Before the analysis of damage detection results, it would be appropriate to investigate the effect of the number of measured modes on the improved sensitivity matrix of MSE. On this basis, one assumes that the sets of 5, 10, 15, and 21 measured modes are available. Figs. 2 and 3 show the observations of this analysis on the improved sensitivity matrix in the damage cases 1 and 2, respectively.

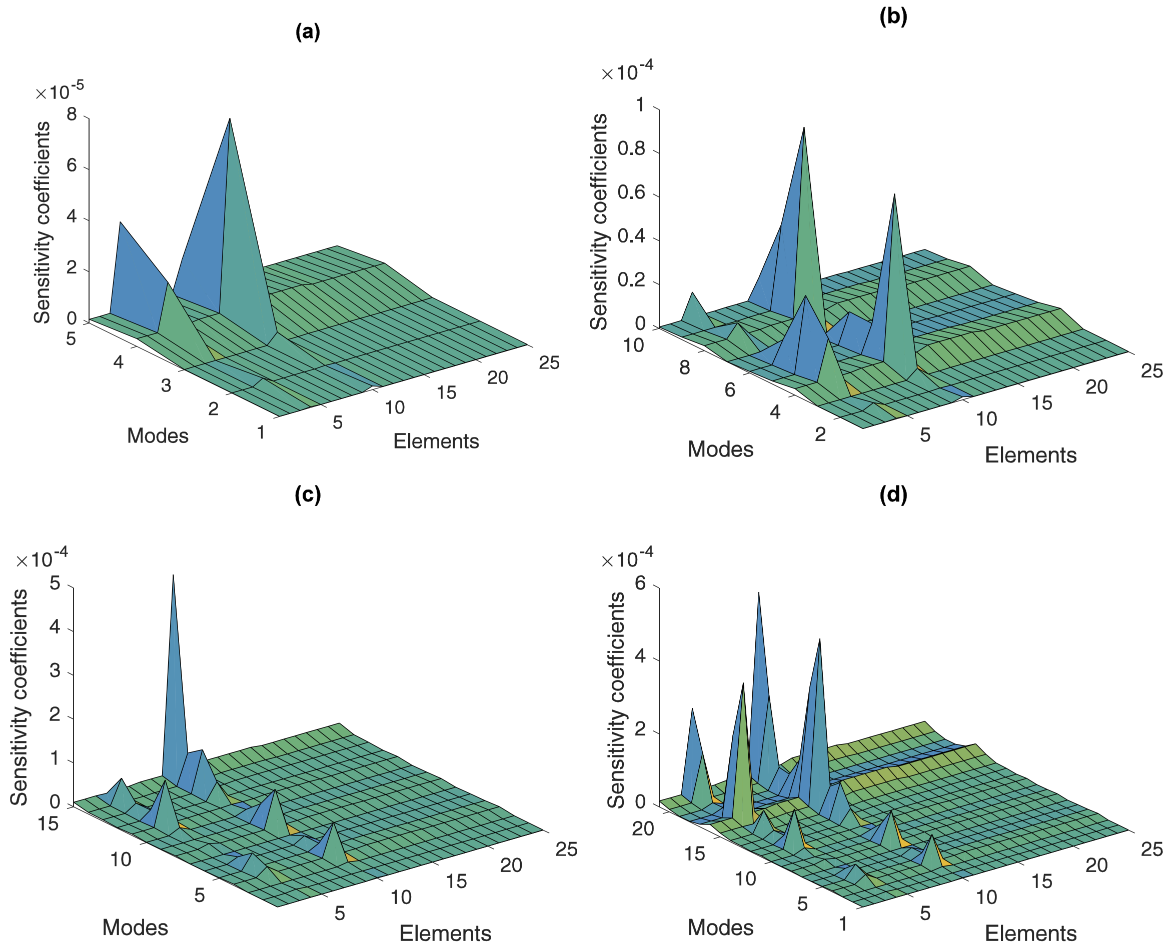

Fig. 2. The effect of measured modes on the improved sensitivity matrix of MSE in the damage case 1: (a) the first five modes, (b) the first ten modes, (c) the first fifteen modes, (d) the complete modes.

As can be seen from these figures, the absolute coefficients of sensitivity matrix at the damaged elements of the truss structure increase with increasing the number of measured modes. This means that the improved sensitivity function of MSE provides a better observation in detecting damage by measuring further modes. This conclusion can simply be proved by the comparison of results between the first five modes, Figs. 2(a) and 3(a), and the complete measured modes, Figs. 2 (d) and 3(d). As another observation, it is obvious from the figures that the damaged elements in both cases have the tallest peaks compared with the other undamaged elements in the truss structure. Thus, it can be argued that the improved sensitivity of MSE is very sensitive to damage even if the small damage occurs in the structure.

6.2. Detectability of damage by sensitivity matrix

The damage detectability by sensitivity matrix is a useful tool to realize which structural elements suffer from damage and which are not. Although the observations in Figs. 2 and 3 demonstrate the capability of the improved sensitivity function in detecting damage, some elements may not be detectable, particularly in the case of using a few modes. In order to assess the ability of sensitivity matrix of MSE to detect structural damage, a detectability index (D) is defined as follows [19]:

$$\boldsymbol{D}_j = \|\mathbf{s}_j\|_2 \tag{68}$$

where $\|.\|_2$ is representative of l_2-norm and $\mathbf{s}_j$ denotes the j^{th} column of the sensitivity matrix, $j = 1,2,\ldots,ne$. A damaged element with a large detectability index can be simply identified, whereas elements with small values of detectability index are almost undamaged areas in the structure. The great merit of detectability index is that it provides a reasonable criterion to identify damage locations without solving the damage equation by any mathematical technique. A comparative analysis on the initial and improved sensitivity functions of MSE is conducted to demonstrate the performance of these sensitivity functions in detecting structural damage. Figs. 4 and 5 show the values of detectability index for the damage cases 1 and 2 considering the first five modes, respectively.

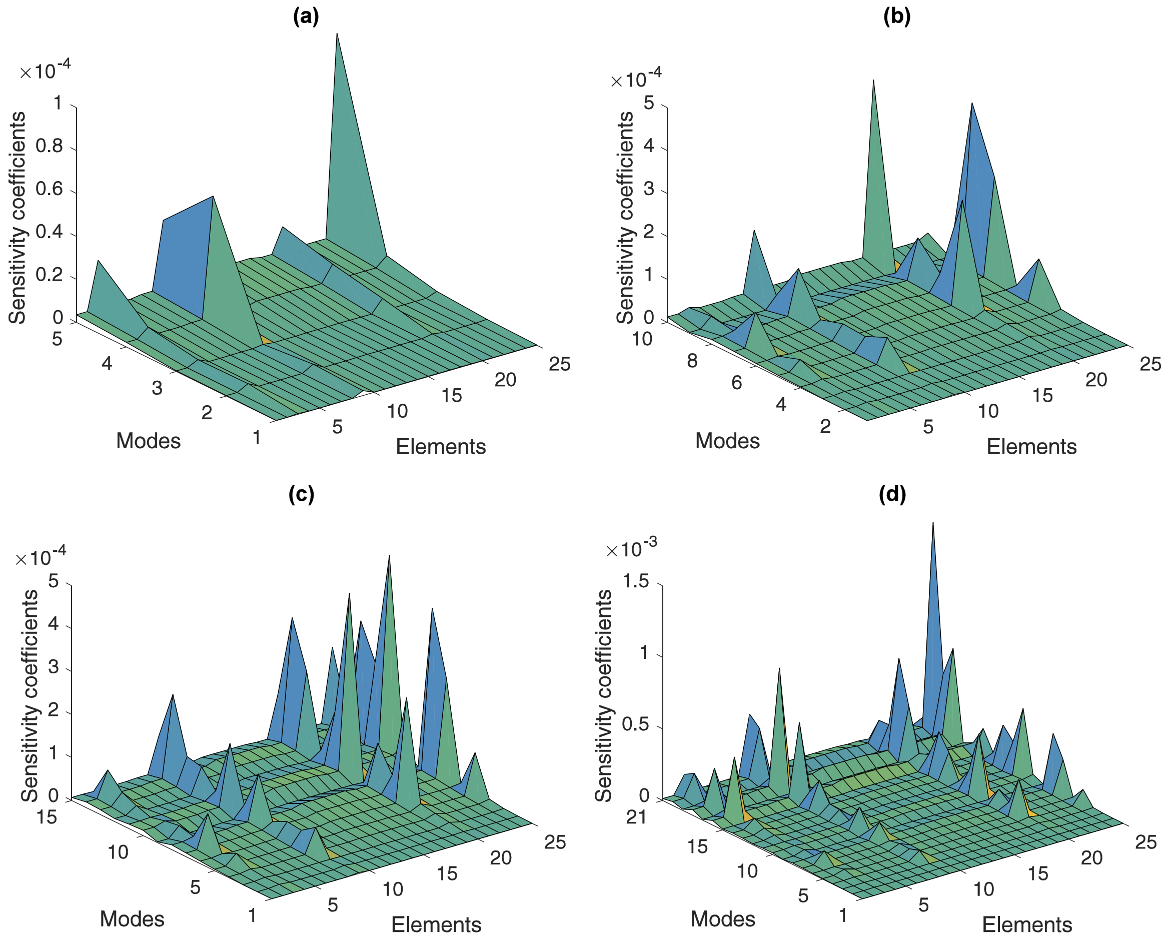

Fig. 3. The effect of measured modes on the improved sensitivity of matrix MSE in the damage case 2: (a) the first five modes, (b) the first ten modes, (c) the first fifteen modes, (d) the complete modes.

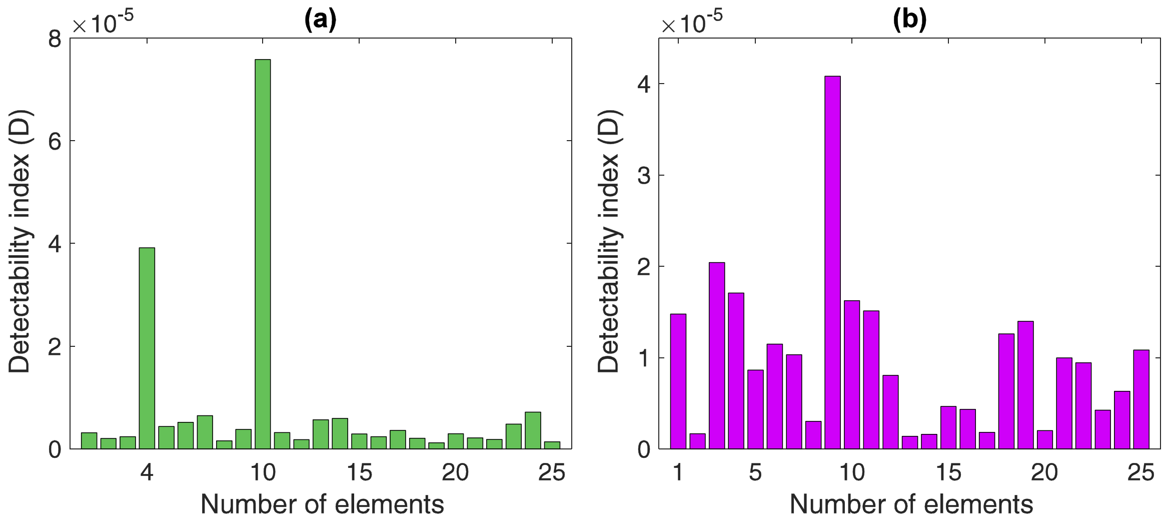

Fig. 4. The detectability of damage in the case 1: (a) the improved sensitivity of MSE, (b) the initial sensitivity of MSE.

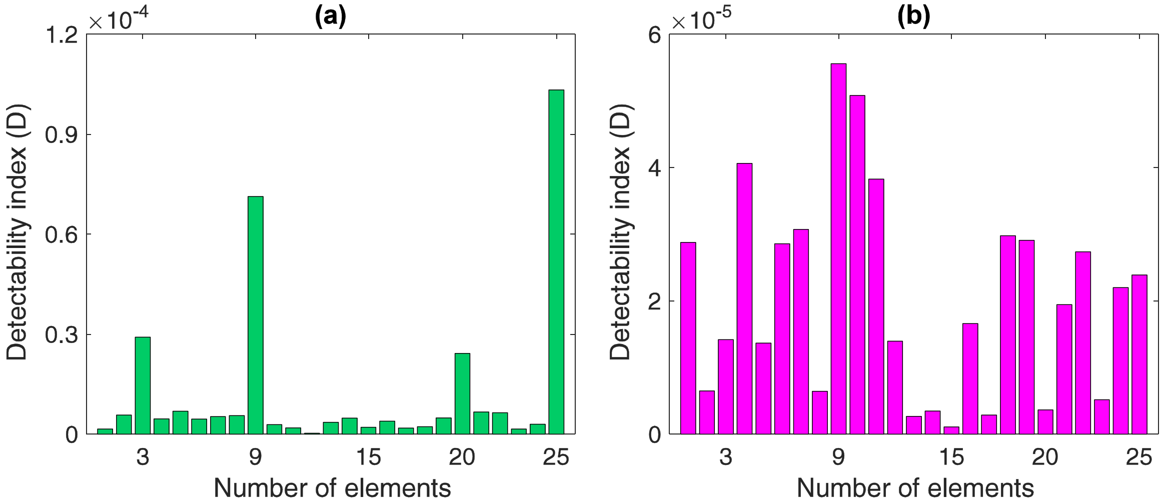

Fig. 5. The detectability of damage in the case 2: (a) the improved sensitivity of MSE, (b) the initial sensitivity of MSE.

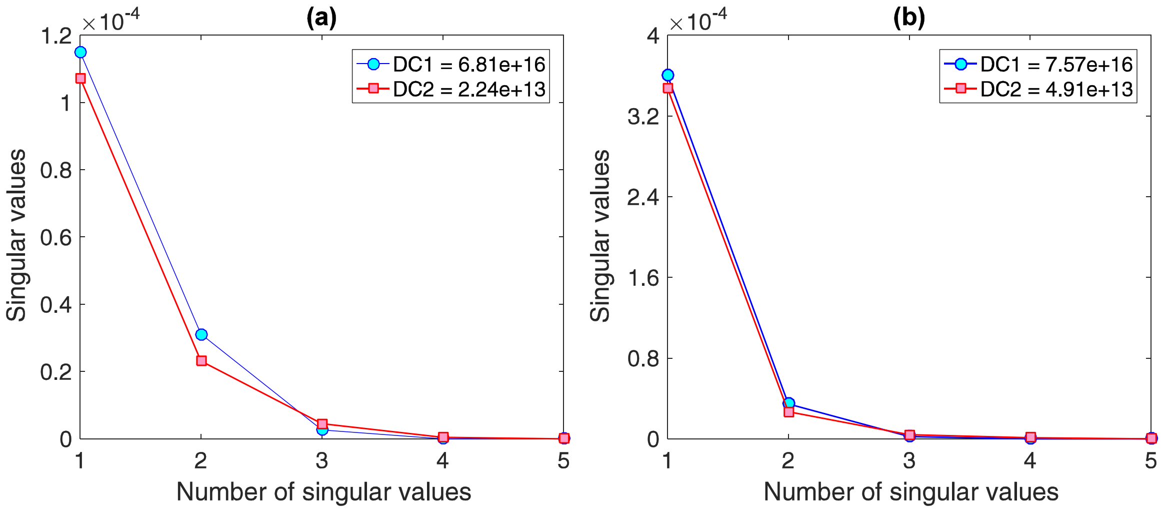

Fig. 6. The evaluation of ill-posed problem for the damage equation in: (a) 1% noise level, (b) 5% noise level (DC: Damage Case).

Fig. 4(a) indicates the amounts of detectability index in the damage case 1 using the improved sensitivity of MSE. It is apparent from the figure that the elements 4 and 10 are indicative of the locations of damage due to the largest quantities of detectability index at these areas compared to the other truss elements. Based on Table 3, the stiffness reduction factors in the damage case 1 have been applied to these elements implying the locations of damage. Fig. 4(b) shows the values of detectability index obtained from the initial sensitivity of MSE. As this figure reveals, there are unclear and false observations in detecting damage.

Fig. 5(a) illustrates the quantities of detectability index gained by the improved sensitivity of MSE in the damage case 2. It is seen that the values of detectability index at the elements 3, 9, 20, and 25 are much more than the other elements, which means that these areas of the truss structure are damage locations. The results of detectability index using the initial sensitivity of MSE in the damage case 2 is shown in Fig. 5(b). In a similar way to the previous damage case, the amounts of detectability index at the elements 3, 20, and 25 cannot clearly suggest the locations of damage with the exception of the element 9. Consequently, the results obtained from Figs. (4) and 5 lead to the conclusions that the improved sensitivity of MSE is sensitive to damage and provides much more appropriate damage detectability results in comparison with the initial sensitivity function.

6.3. Evaluation of ill-posed problem

The majority of damage identification methods are ill-posed problems. An ill-posed problem has two specific

Table 4
The number of iterations required by the RLSMR method.

Case no.	Noise level (%)	
	1	5
1	23	34
2	29	41

Table 5
The optimal regularization parameters in the different noise levels.

Method	Case no.	Noise level (%)	
		1	5
RLSMR	1	57.81e-4	70.22e-4
	2	61.97e-4	88.14e-4
Tikhonov	1	46.93e-6	66.21e-6
	2	50.81e-6	54.06e-6

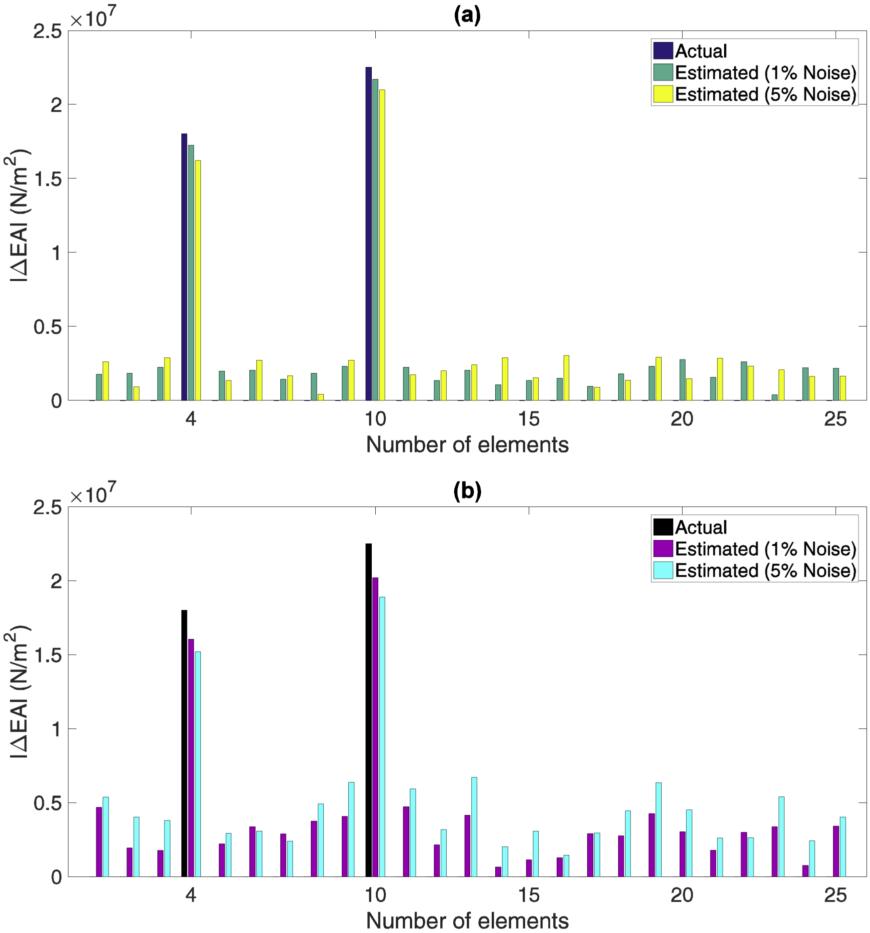

Fig. 7. Damage localization and quantification by the incomplete noisy modal parameters in the damage case 1: (a) RLSMR method, (b) Tikhonov regularization method.

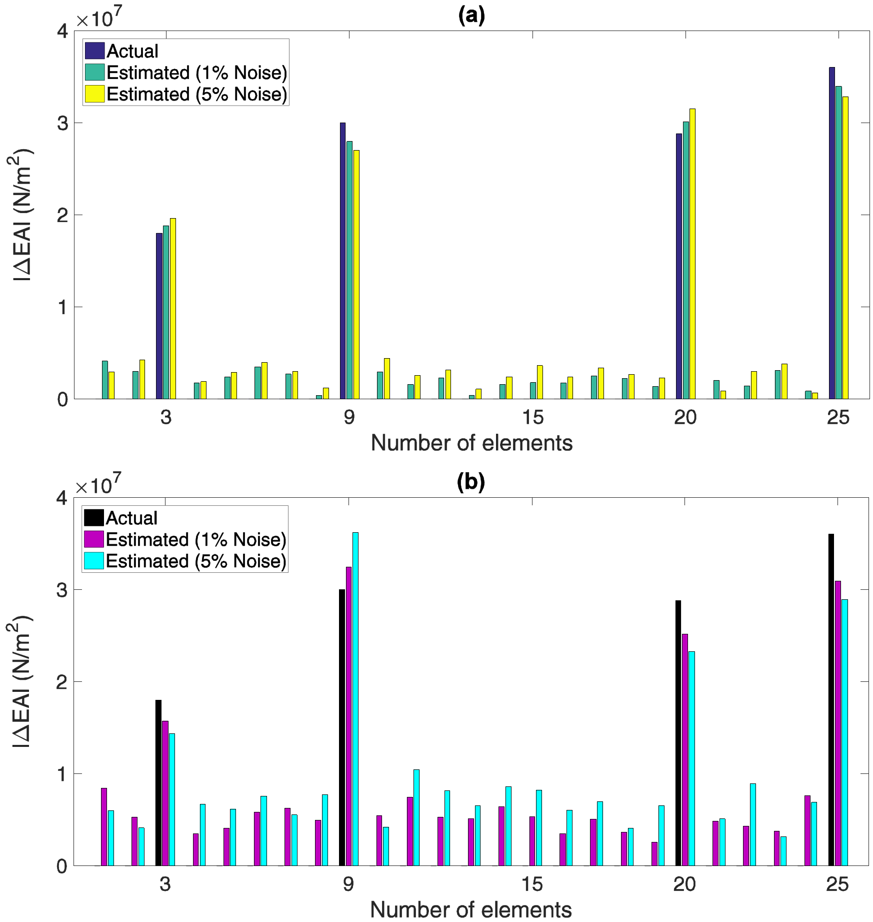

Fig. 8. Damage localization and quantification by the incomplete noisy modal parameters in the damage case 2: (a) RLSMR method, (b) Tikhonov regularization method.

characteristics: (i) the singular values of sensitivity matrix decay gradually to zero, and (ii) the ratio between the largest and smallest non-zero singular values of the sensitivity matrix is large [44]. This ratio implies that the sensitivity matrix is ill-conditioned; that is, the solution of linear system is very sensitive to small perturbations such as measurement errors in the modal data. This section aims to ascertain whether the damage equation is an ill-posed problem. On this basis, two different noise levels are utilized to simulate measurement errors including: (i) 1% noise level, and (ii) 5% noise level. The simulation of noisy modal data in most numerical problems is carried out by adding a sequence of random numbers as Gaussian distribution with zero mean in the following forms:

$$\hat{\boldsymbol{\varphi}}_i^* = \left(1 + \mu_i \eta\right)\hat{\boldsymbol{\varphi}}_i \tag{69}$$

$$\hat{\lambda}_i^* = \left(1 + \mu_i \eta\right)\hat{\lambda}_i \tag{70}$$

where $\hat{\boldsymbol{\varphi}}_i^*$ and $\hat{\boldsymbol{\varphi}}_i$denote the ith noisy and noise-free measured eigenvectors (the mass-normalized mode shapes of the tested structure), respectively. Additionally, $\hat{\lambda}_i^*$ and $\hat{\lambda}_i$ are the ith noisy and noise-free measured eigenvalues. In these equations, η represents the noise level and μ is a Gaussian random sequence with zero mean. Assume that the mode shapes of the structure in the undamaged condition are contaminated by noise. Fig. 6 shows the singular values of the improved sensitivity matrix of MSE by considering the two different noise levels.

As can be seen, the singular values tend to decay gradually to zero in both damage cases. Furthermore, the condition numbers of the improved sensitivity matrix are large quantities. Such observations prove that the damage equation is an ill-posed problem. It is also seen in this figure that increasing the level of noise, the singular values of sensitivity matrix more tend to decay gradually to zero. This conclusion is concerned with the effect of perturbation on the solution of damage equation. It is worth remarking that the sensitivity matrix is a 5-by-25 rectangular matrix, where 5 denotes the number of measured modes (m) and 25 implies the number of elements (n_e). Since $m < ne$; therefore, the only five singular values obtained by the SVD technique are usable.

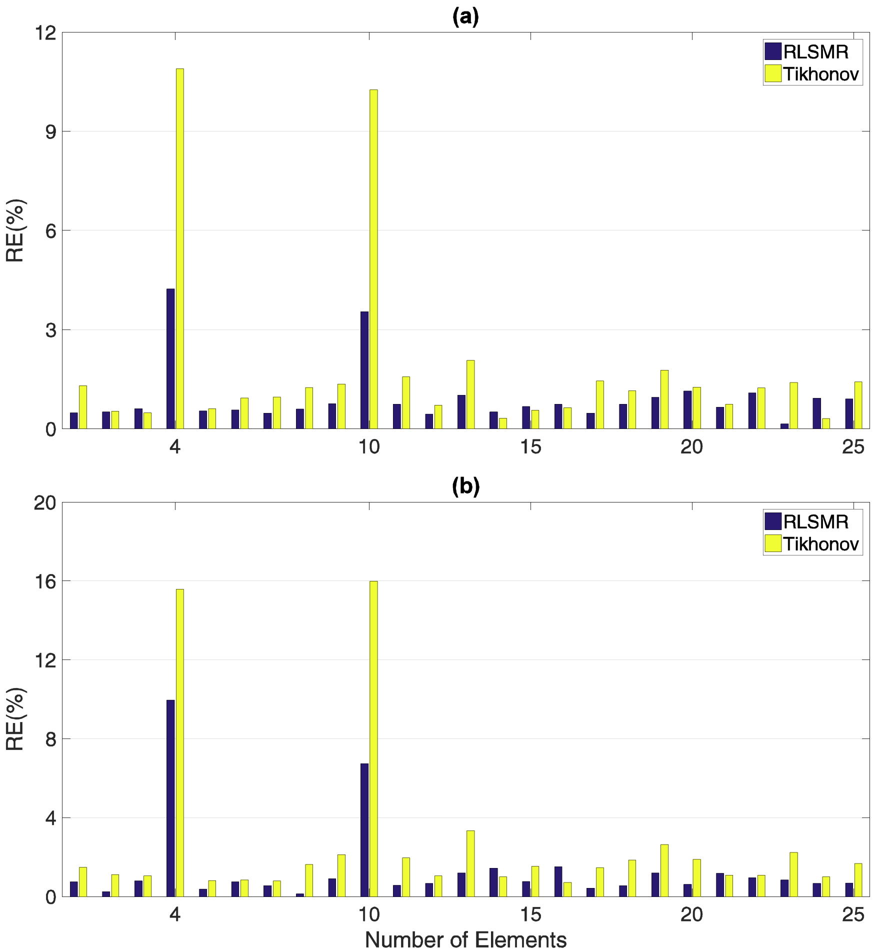

Fig. 9. The relative errors in damage quantities for the damage case 1: (a) 1% noisy data, (b) 5% noisy data.

6.4. *Damage detection using incomplete noisy modal data*

In this section, the process of damage detection is implemented by the improved sensitivity of MSE, the RLSMR method, and the hybrid technique. The term of damage detection refers to identify the damage locations (the process of damage localization) and estimate the damage severity (the process of damage quantification). Despite superior ability of the improved sensitivity of MSE to identify damage locations by the detectability index, this process may fail to yield robust and proper results when the modal parameters are contaminated by noise. Furthermore, it is important to estimate damage severity, because the detectability index is not generally able to perform the process of damage quantification. Therefore, there is a great necessity to solve the ill-posed damage equation by the RLSMR method. For a comparative study, the results of damage localization and quantification gained by the RLSMR method along with the hybrid GCV function are compared with the corresponding results of Tikhonov regularization method incorporating the conventional GCV function.

In order to determine the optimal regularization value by the hybrid method, one significant characteristic is the number of iterations required by the RLSMR method for the regularized solution of ill-posed damage equation. Table 4 presents the iterations of RLSMR method for the regularized solution in the two noise levels.

The information in Table 4 indicates that the number of iterations increases with increasing the level of noise, the number of damaged elements, and the severity of damage. Moreover, there are reasonable iterations throughout the regularized solution of damage equation in all noise levels. These conclusions demonstrate that the RLSMR method with a good estimation of regularization parameter converges to a stable solution with acceptable iterations. Note that the stopping condition for the termination of iterations in the algorithm of RLSMR corresponds to 1.0e-5. Once the iterations of RLSMR method have been determined, the optimal regularization values concerning the noise levels and both damage cases are gained by the hybrid GCV function presented in Eq. (67). Furthermore, the optimal regularization quantities for the Tikhonov regularization technique are computed by the conventional GCV function as formulated in Eq. (66). Table 5 represents the regularization parameters for the RLSMR and Tikhonov methods.

The process of determining the regularization value using the GCV functions starts with a high regularization value. The

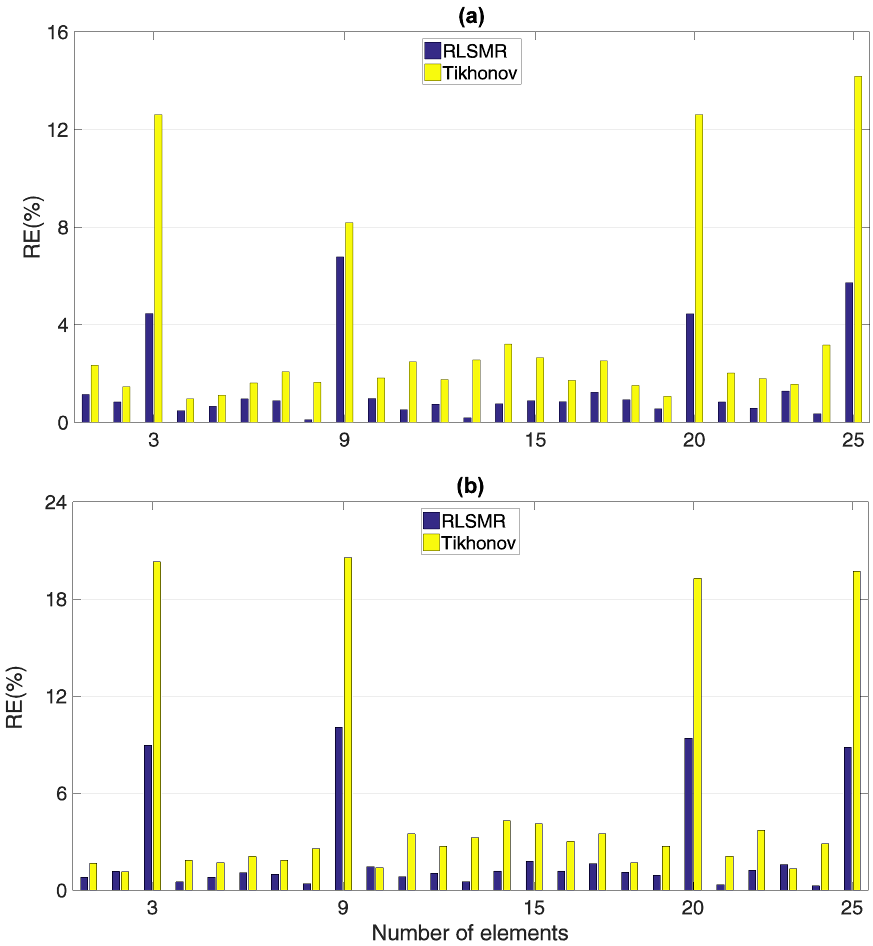

Fig. 10. The relative errors in damage quantities for the damage case 2: (a) 1% noisy data, (b) 5% noisy data.

Table 6
The number of iterations and optimal regularization parameters needed to the RLSMR method by considering the mass modeling errors.

Case no.	Index	Mass modeling errors (%)		
		1	5	10
1	Iteration no.	16	16	20
	γ	25.11e-4	22.87e-4	37.71e-4
2	Iteration no.	18	19	23
	γ	38.11e-4	44.90e-4	51.29e-4

optimal regularization parameter is one that the GCV function to be minimized. From Table 5, one can realize that the regularization amounts increase with increasing the noise levels and the damage extents.

Figs. 7 and 8 indicate the results of damage localization and quantification using the incomplete noisy modal parameters in the damage cases 1 and 2 respectively. In each figure, the results obtained by the RLSMR method are compared with the Tikhonov regularization method. It is worth noting that the vertical coordinate of these figures is identical to the absolute amounts of discrepancy axial rigidity (ΔEA). As Figs. 7(a) and 8(a) appear, the locations of damage are precisely identified by the RLSMR method in both noise levels. The same conclusion can be achieved based on the Tikhonov regularization method as illustrated in Figs. 7(b) and 8(b). It is significant to point out that one of the main reasons of precise damage localization results in both regularization methods is pertinent to the improved sensitivity of MSE and its great damage detectability.

From the results of damage quantification obtained by the RLSMR method, one can satisfy that this method is reasonably capable of quantifying damage in the presence of incomplete noisy modal parameters and ill-conditioned sensitivity matrix. Furthermore, it can be seen from Figs. 7(a) and 8(a) that the false estimations of damage severities at the undamaged elements are nearly inconsiderable value. Another observation in these figures is that the levels of noise do not have any effects on the process of damage localization and quantification. The comparison of results in the process of damage

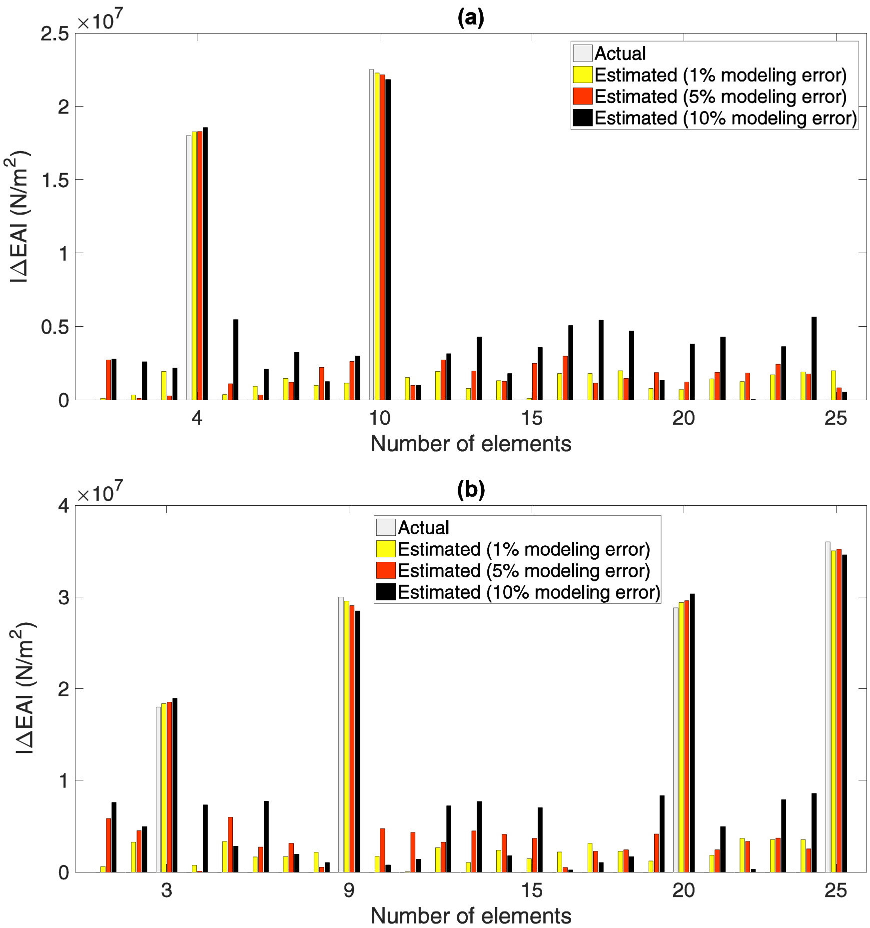

Fig. 11. Damage localization and quantification using the improved sensitivity of MSE and the RLSMR method by considering the mass modeling errors: (a) case 1, (b) case 2.

quantification indicates that the false estimations of damage quantifies by the Tikhonov regularization method are much more than the corresponding estimations gained by the RLSMR method. Moreover, one can observe that there are approximately large computational errors in the estimated damage severities obtained from the Tikhonov regularization method, particularly in the 5% noise level. For a better comparative process, Figs. 9 and 10 illustrate the relative errors in damage quantities for the damage cases 1 and 2, respectively.

The observations in these figures appear that the relative errors in the damage quantities of Tikhonov regularization method increase with increasing the noise levels so that there are relatively large errors (approximately near to 20% for the case 2) in the quantification of damage. On the contrary, the RLSMR method yields proper results with the small relative errors in such a way that the largest error corresponds to 10.07% for the 5% noise level. As a result, the observations in Figs. 7–10 evidence the superiority of RLSMR method along with the hybrid GCV function over the Tikhonov regularization technique by incorporating the conventional GCV function in quantifying damage.

6.5. Modeling errors

A damage detection problem based on model updating strategy might be impacted by critical issues such as incomplete measurements, damage detectability, noisy data, and modeling errors. In most cases, it is assumed that the FE model of the structure, which refers to the original or undamaged state, has been updated and calibrated by model updating techniques [18]. However, it is possible to encounter uncertainties in modeling of the FE model such as an inaccurate estimation of mass matrix. For the majority of real cases, structural damage does not affect the mass parameters; however, an unreliable and inaccurate assumption of mass properties may introduce some errors in estimating the mode shapes and natural frequencies of FE model, which are used to construct the sensitivity matrix [18,35,36]. In order to simulate such uncertainties in the damage detection problem, three different modeling errors including 1, 5, and 10% of uniformly distributed mass errors are separately added to all individual elements. The number of iterations and the optimal regularization values needed to the RLSMR method are presented in Table 6.

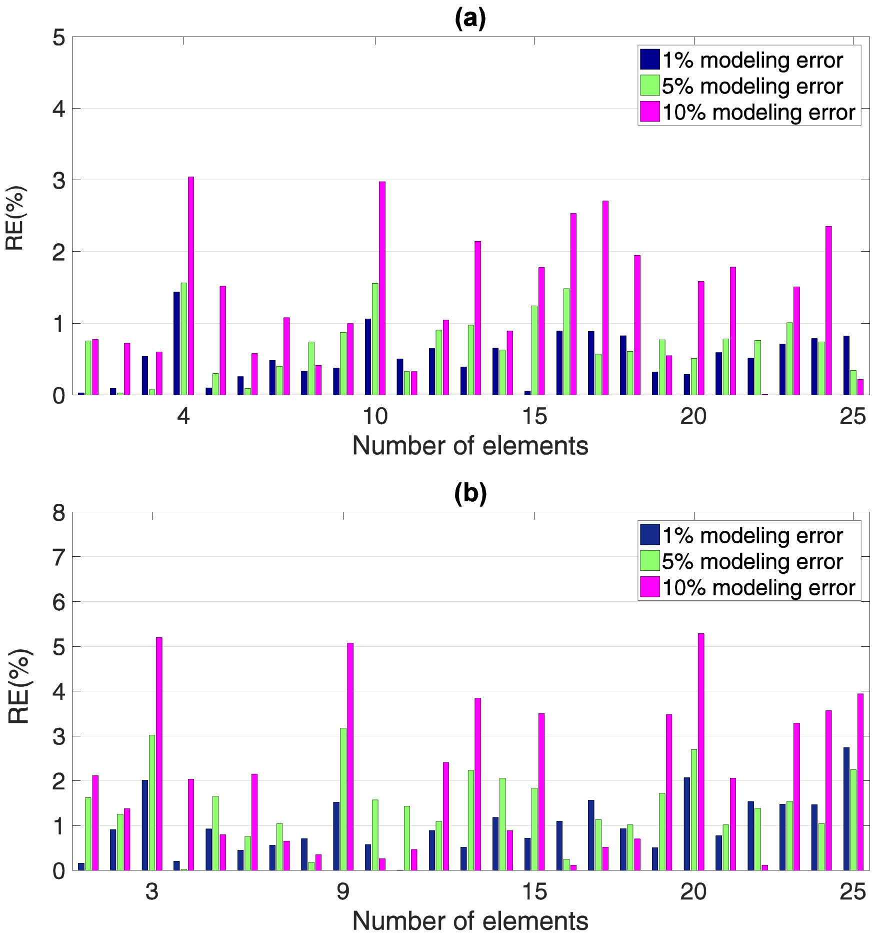

Fig. 12. The relative errors in damage quantities by considering the mass modeling errors: (a) case 1, (b) case 2.

With such information, Fig. 11 shows the results of damage localization and quantification in both damage cases in the presence of mass modeling errors.

From this figure, one can discern that there are acceptable results in detecting damage even in the presence of modeling errors. Additionally, it is seen that the locations of damage are precisely identified by the improved and proposed methods. For the procedure of damage quantification, there are accurate estimations with inconsiderable computational errors at the damaged elements. In both damage cases, the false damage quantities at the undamaged elements are very small amounts in the 1 and 5% mass modeling errors. In the 10% modeling error, the false estimation of damage quantities at the undamaged elements increase; however, these amounts are not comparable with their corresponding values at the damaged elements.

The relative errors in damage quantities by considering the mass modeling errors are shown in Fig. 12. It can be perceived from this figure that the errors are nearly less than 3% and 5% for the damage cases 1 and 2, respectively. Therefore, there is sufficient evidence to demonstrate the accuracy of damage detection results in the presence of mass modeling errors.

7. Conclusions

In this article, a new sensitivity-based damage detection method has been proposed to identify damage location and estimate damage severity using the incomplete noisy modal parameters and FE modeling errors. An improved sensitivity function of MSE has been developed to establish a sensitivity formulation regarding the damage detection problem using the Lagrange optimization problem with the new mathematical approaches. To solve the ill-posed damage identification equation, the new iterative regularization method (RLSMR) has been introduced. The performance of this method in the damage detection problem has been compared with the well-known Tikhonov regularization method. The hybrid technique has then been presented to determine the optimal regularization parameter. Eventually, the accuracy and reliability of the improved and proposed methods have numerically been demonstrated by the well-known planner truss. A comparative study on the initial and improved sensitivity functions of MSE has also been conducted to evaluate the capability of damage detectability by these functions.

The numerical results showed that: (1) The improved sensitivity function of MSE is very sensitive to damage based on the obtained values of detectability index. (2) The detectability of damage by the improved sensitivity function demonstrated that it is able to locate damage. (3) The comparison of the initial and improved sensitivity functions indicated that the improved sensitivity of MSE has a robust damage detectability, whereas the initial sensitivity function fails to detect damage. (4) Both RLSMR and Tikhonov methods are capable of locating structural damage in all noise levels. (5) The accuracy of damage localization results depends strongly on the improved sensitivity function of MSE. (6) The comparison of these methods in the process of damage quantification showed that the RLSMR method provide better results than the Tikhonov regularization method. (7) The RLSMR method solves the damage equation with a few and plausible iterations in such a way that the highest noise level makes most iterations. (8) Taking the mass modeling errors into accounts, the improved sensitivity of MSE and RLSMR method are influentially able to identify damage location and estimate damage quantity.

References

[1] S.W. Doebling, C.R. Farrar, M.B. Prime, A summary review of vibration-based damage identification methods, *Shock Vib. Dig.* 30 (1998) 91–105.
[2] J.T. Kim, N. Stubbs, Crack detection in beam-type structures using frequency data, *J. Sound Vib.* 259 (2003) 145–160.
[3] Z.R. Lu, J.K. Liu, M. Huang, W.H. Xu, Identification of local damages in coupled beam systems from measured dynamic responses, *J. Sound Vib.* 326 (2009) 177–189.
[4] M.A.B. Abdo, M. Hori, A numerical study of structural damage detection using changes in the rotation of mode shapes, *J. Sound Vib.* 251 (2002) 227–239.
[5] A. Pandey, M. Biswas, M. Samman, Damage detection from changes in curvature mode shapes, *J. Sound Vib.* 145 (1991) 321–332.
[6] Z. Shi, S. Law, L. Zhang, Damage localization by directly using incomplete mode shapes, *J. Eng. Mech.* 126 (2000) 656–660.
[7] A. Rahai, F. Bakhtiari-Nejad, A. Esfandiari, Damage assessment of structure using incomplete measured mode shapes, *Struct. Control Health Monit.* 14 (2007) 808–829.
[8] E. Simoen, G. De Roeck, G. Lombaert, Dealing with uncertainty in model updating for damage assessment: a review, *Mech. Syst. Signal Process.* 56 (2015) 123–149.
[9] J.E. Mottershead, M. Link, M.I. Friswell, The sensitivity method in finite element model updating: a tutorial, *Mech. Syst. Signal Process.* 25 (2011) 2275–2296.
[10] H.F. Lam, J.M. Ko, C.W. Wong, Localization of damaged structural connections based on experimental modal and sensitivity analysis, *J. Sound Vib.* 210 (1998) 91–115.
[11] B.H. Koh, S.J. Dyke, Structural health monitoring for flexible bridge structures using correlation and sensitivity of modal data, *Comput. Struct.* 85 (2007) 117–130.
[12] H. Zhu, L. Li, X.-Q. He, Damage detection method for shear buildings using the changes in the first mode shape slopes, *Comput. Struct.* 89 (2011) 733–743.
[13] A. Esfandiari, F. Bakhtiari-Nejad, A. Rahai, Theoretical and experimental structural damage diagnosis method using natural frequencies through an improved sensitivity equation, *Int. J. Mech. Sci.* 70 (2013) 79–89.
[14] W.J. Yan, W.X. Ren, A direct algebraic method to calculate the sensitivity of element modal strain energy, *Int. J. Numer. Methods Biomed. Eng.* 27 (2011) 694–710.
[15] W.J. Yan, W.X. Ren, T.L. Huang, Statistic structural damage detection based on the closed-form of element modal strain energy sensitivity, *Mech. Syst. Signal Process.* 28 (2012) 183–194.
[16] L. Li, Y. Hu, X. Wang, Numerical methods for evaluating the sensitivity of element modal strain energy, *Finite Elem. Anal. Des.* 64 (2013) 13–23.
[17] P.C. Hansen, *Rank-Deficient and Discrete Ill-Posed Problems: Numerical Aspects of Linear Inversion*, SIAM, 1998.
[18] H.-P. Chen, Application of regularization methods to damage detection in large scale plane frame structures using incomplete noisy modal data, *Eng. Struct.* 30 (2008) 3219–3227.
[19] B. Weber, P. Paultre, J. Proulx, Consistent regularization of nonlinear model updating for damage identification, *Mech. Syst. Signal Process.* 23 (2009) 1965–1985.
[20] X. Li, S. Law, Adaptive Tikhonov regularization for damage detection based on nonlinear model updating, *Mech. Syst. Signal Process.* 24 (2010) 1646–1664.
[21] H.-P. Chen, T.S. Maung, Regularised finite element model updating using measured incomplete modal data, *J. Sound Vib.* 333 (2014) 5566–5582.
[22] M. Aucejo, Structural source identification using a generalized Tikhonov regularization, *J. Sound Vib.* 333 (2014) 5693–5707.
[23] N. Grip, N. Sabourova, Y. Tu, Sensitivity-based model updating for structural damage identification using total variation regularization, *Mech. Syst. Signal Process.* 84 (Part A) (2017) 365–383.
[24] H.-P. Chen, Mode shape expansion using perturbed force approach, *J. Sound Vib.* 329 (2010) 1177–1190.
[25] F. Liu, Direct mode-shape expansion of a spatially incomplete measured mode by a hybrid-vector modification, *J. Sound Vib.* 330 (2011) 4633–4645.
[26] M. Friswell, J.E. Mottershead, *Finite Element Model Updating in Structural Dynamics*, Springer, Netherlands, 1995.
[27] R.J. Guyan, Reduction of stiffness and mass matrices, *AIAA J.* 3 (1965) 380.
[28] R.L. Kidder, Reduction of structural frequency equations, *AIAA J.* 11 (1973) 892.
[29] J.C. O'Callahan, P. Avitabile, R. Riemer, System equivalent reduction expansion process, in: Proceedings of the Seventh International Modal Analysis Conference, Las Vegas, Nevada, USA, 1989.
[30] J. Snyman, *Practical Mathematical Optimization: an Introduction to Basic Optimization Theory and Classical and New Gradient-Based Algorithms*, Springer, 2005.
[31] S.S. Rao, *Engineering Optimization: theory and Practice*, Wiley, 2009.
[32] J.S. Arora, *Optimization of Structural and Mechanical Systems*, World Scientific, 2007.
[33] I. Ekeland, On the variational principle, *J. Math. Anal. Appl.* 47 (1974) 324–353.
[34] J.S. Arora, J.B. Cardoso, Variational principle for shape design sensitivity analysis, *AIAA J.* 30 (1992) 538–547.
[35] A. Esfandiari, An innovative sensitivity-based method for structural model updating using incomplete modal data, *Struct. Control Health Monit.* (2016).
[36] M. Farshadi, A. Esfandiari, M. Vahedi, Structural model updating using incomplete transfer function and modal data, *Struct. Control Health Monit.* (2016).
[37] D. Fong, M. Saunders, LSMR: an Iterative Algorithm for Sparse Least-Squares Problems, *SIAM J. Sci. Comput.* 33 (2011) 2950–2971.
[38] H. Sarmadi, A. Karamodin, A. Entezami, A new iterative model updating technique based on least squares minimal residual method using measured modal data, *Appl. Math. Model.* 40 (2016) 10323–10341.
[39] G. Golub, W. Kahan, Calculating the singular values and pseudo-inverse of a matrix, *J. Soc. Ind. Appl. Math. Ser. B Numer. Anal.* 2 (1965) 205–224.
[40] C.C. Paige, M.A. Saunders, LSQR: an algorithm for sparse linear equations and sparse least squares, *ACM Trans. Math. Softw. (TOMS)* 8 (1982) 43–71.
[41] H. Ahmadian, J. Mottershead, M. Friswell, Regularisation methods for finite element model updating, *Mech. Syst. Signal Process.* 12 (1998) 47–64.
[42] X. Hua, Y. Ni, J. Ko, Adaptive regularization parameter optimization in output-error-based finite element model updating, *Mech. Syst. Signal Process.* 23 (2009) 563–579.
[43] M.E. Kilmer, D.P. O'Leary, Choosing regularization parameters in iterative methods for ill-posed problems, *SIAM J. Matrix Anal. Appl.* 22 (2001) 1204–1221.
[44] P.C. Hansen, Regularization tools: a Matlab package for analysis and solution of discrete ill-posed problems, *Numer. Algorithms* 6 (1994) 1–35.
[45] D.P. O'Leary, J.A. Simmons, A bidiagonalization-regularization procedure for large scale discretizations of ill-posed problems, *SIAM J. Sci. Stat. Comput.* 2 (1981) 474–489.
[46] A. Esfandiari, F. Bakhtiari-Nejad, A. Rahai, M. Sanayei, Structural model updating using frequency response function and quasi-linear sensitivity equation, *J. Sound Vib.* 326 (2009) 557–573.
[47] A. Esfandiari, Structural model updating using incomplete transfer function of strain data, *J. Sound Vib.* 333 (2014) 3657–3670.
[48] X. Gang, S. Chai, R.J. Allemang, L. Li, A new iterative model updating method using incomplete frequency response function data, *J. Sound Vib.* 333 (2014) 2443–2453.